A Study of Rubberfatigue Life and Cure Parameters

Jack Alberts
Marquette University

A STUDY OF RUBBER FATIGUE LIFE AND CURE PARAMETERS

by

Jack Alberts

A Thesis Submitted to the Faculty of the Graduate School,
Marquette University,
in Partial Fulfillment of the Requirements for
the Degree of Master of Science

Milwaukee, Wisconsin

December 2018

ABSTRACT
A STUDY OF RUBBER FATIGUE LIFE AND CURE PARAMETERS

Jack Alberts

Marquette University, 2018

There is demand for increasing rubber life in parts within medium and heavy duty suspension systems. Rubber plays a major factor in lightening the overall weight of the suspension system; therefore, increasing the hauling capacity of the truck. This thesis focused on optimizing the cure time and cure temperature of the manufacturing process as it relates to the fatigue life of rubber suspension parts. Samples of rubber parts were made using molding techniques with different process parameters, specifically cure time and temperature. These samples then underwent a series of nondestructive tests, to quantify, for example, dynamic stiffness, and then a destructive test, to quantify fatigue life. Multiple analytical approaches were then used to determine the process parameters that produced the rubber components with the highest fatigue life. Similarly, regression models were utilized to predict fatigue life based on nondestructive test results. The fatigue testing had to be terminated prematurely due to inconsistent fatigue results based on the failure mechanism of the samples. However, the design of experiment created and the analysis techniques used in this thesis will be the basis for future experiments performed on new rubber products.

ACKNOWLEDGEMENTS

Jack Alberts

I would first off like to thank Dr. Philip A. Voglewede for providing me with advice and guidance. This work could not have been completed without his support. In addition, I would like to thank my committee members, Dr. James Rice and Dr. Ting Lin, for their continuous support throughout my research and development of this work. Finally, I would like to thank my friends and family for their love and encouragement.

TABLE OF CONTENTS

CHAPTER 1

Introduction

Through decades of research into formulation and processing, engineers have developed natural rubber into a durable engineered material with a high elastic modulus and yield strength; therefore, rubber can be put under large static loads as well as smaller dynamic loads. Rubber's ability to handle large loads and its resistance to wear and fatigue make it suitable for cyclic loading applications. Some applications for rubber include tires, seals, and footwear.

The rubber application studied in this thesis is for medium and heavy-duty suspension systems, specifically in commercial trucks. The transition from steel components to rubber components is to reduce the overall weight of the suspension system. Lighter suspensions translate into lighter trucks, which in turn translates into better fuel economy.

These rubber components not only decrease the weight of the overall suspension system, but also have a damping effect, which provides a smoother ride for the driver. Rubber fatigue analysis is not as well documented in suspension systems as their steel counterparts. Therefore, this thesis focuses on fatigue analysis of the rubber components, with an emphasis on the correlation with the molding process.

The molding process for rubber has a significant impact on the fatigue life of the rubber. Although there are many variables that affect the performance, such as environmental conditions and rubber chemistry, only the controlled parameters of the manufacturing process were investigated to understand their effect on fatigue

performance. The geometry is not investigated because the geometry is already established within each of the suspension systems. This establishment means that the package space is well defined and rigid, and the package space often limits the size of the molded rubber product.

The objective of this study is to optimize the manufacturing parameters to maximize the fatigue life of rubber components. There are several factors that characterize a successful part, such as stiffness or hardness, but the criteria of interest is lengthening the overall life of their rubber parts.

CHAPTER 2

Literature Review

Rubber fatigue analysis is not a new concept. There are numerous research studies that focus on the fundamentals of why rubber fails due to cyclic loading. The fundamental basis of why rubber fails is due to its intrinsic flaws, one being microscopic cracks [1]. These flaws can be the result of the inconsistencies in the molding process. In other words, the rubber is not uniform throughout when molded. Because the rubber components have significant volume, an aspect of variability is that the inside of the rubber may have different elastic properties than rubber near the outer walls due to temperature gradients in the rubber during the molding process. Therefore, flaws occur, and the failure mechanism under cyclic loading is the nucleation and propagation of those flaws [1].

The fundamental theory of fatigue failure states that under repeated deformations, failure will occur [1]. This definition is different than static failure, where an object fails under a large static load. For example, a rubber band may be slowly stretched until it snaps; this failure would be considered static failure. On the other hand, if the rubber band is only stretched to half the distance as it was when static failure occurs, the rubber band can return to its original length (i.e. elastic deformation). However, if that same motion is repeated, the rubber band will eventually fail. This failure is fatigue failure. Chapter 2 will explain several aspects that affect fatigue failure and how it relates to processing and the optimization that will be the focus of this thesis.

2.1 **Rubber Formulation**

Rubber formula variables includes filler type as well as the type and quality of antioxidants, antiozonants, and curatives. Natural rubber (polyisoprene), which comes from the latex of Hevea Bralilensis trees, is mixed with these fillers, antioxidants, etc. and long strands of "virgin" rubber are produced [2] [3]. These strands are then cured in a process called vulcanization where the polymer chains are cross linked with the fillers, antioxidants, etc. and are formed into the desired shape. The vulcanization process provides dimensional stability of the physical properties (e.g. tensile strength, elongation etc.) of the specimen. However, this thesis focuses on the processing of the rubber, not the chemistry of the rubber. Therefore, the material content that makes up the rubber will remain the same.

The primary filler used in rubber is called carbon black. Lake and Lindley [1] observed that carbon black has a profound strengthening effect, depending on the type of carbon black and the volume fraction used. Fillers are usually used to increase tensile strength, hardness, and tearing energy. Unfortunately, fillers usually decrease the fatigue life. For example, Ansarifar, et al. [2] conducted an experiment which showed that silica nanofiller decreased the fatigue life drastically.

Another main filler to natural rubber is sulfur. Sulfur is often the curative that binds the polymer chains during the vulcanization process. Natural rubber becomes a thermoset during the vulcanization process, which means the process cannot be reversed once the rubber is vulcanized. The use of sulfur in the compound greatly improves the rubber's fatigue life because sulfur creates a higher crosslink density in the rubber, thus it takes more energy for the rubber to be broken down. A US patent [3] defines a method

for improving rubber fatigue that includes submerging the cured rubber in a liquid solution of sulfur. This process significantly increased the fatigue life of rubber. Furthermore, as seen in Poh [4], an increase in sulfur content increases the strength of the rubber. A rheometer was used to measure torque while the rubber sample was cured. Ultimately, torque increased with an increase in sulfur content [4].

2.2 Rubber Processing

The major focus for this work is the vulcanization of the rubber. Vulcanization is the process of "curing" the rubber, which is synonymous with "cooking" the rubber. Curing is the process of cross-linking the polymer chains, and once cured, the natural rubber becomes a thermoset. During the molding process, the rubber is injected into the hot mold (around 170°C), and the temperature of the rubber is brought up to a certain point (around 135-140°C). The component then "cures" or "cooks" for a certain amount of time (around 5 to 10 minutes). The molding parameters of time and temperature are known as cure time and cure temperature. Vulcanization creates covalent bonds, otherwise known as crosslinks between the polymer chains. For every rubber formulation, there is an optimum crosslink density to maximize fatigue life. The focus of this thesis is to determine the different combinations of cure time and cure temperature that produce the greatest fatigue life.

Similar to the experiment conducted in this work, Posadas et. al [5] conducted an experiment which monitored the torque on the virgin rubber while curing it by manipulating the cure temperature and a sulfur agent. The temperatures ranged from 90 degrees Celsius to 170 degrees Celsius with 10 degree increments. A rheometer was used to measure the torque while the rubber was being cured. In addition to the torque

measurements, the cure time was also measured. It was concluded that the maximum torque was achieved when the cure temperature was 130 degrees Celsius. Even though this thesis focuses on fatigue life, this experiment is an example of optimization to maximize a quality of the rubber.

2.3 **Mechanical Behavior**

Many researchers [6], [7], [8], [9], [10] have stated that rubber fails under cyclic loading due to the nucleation and growth of cracks. The nucleation stage involves the potential crack growth of many microscopic cracks. The crack growth stage focuses on the development of one of those cracks. Wang et al. [11] determined that the time it takes for a crack to go from the nucleation stage to the crack growth stage may take many loading cycles. On the other hand, the time it takes for a crack to go from the crack growth stage to failure may take very few loading cycles. The nucleation stage and crack growth stage depend on the response of the rubber at different strains as well as the strain rate (i.e. frequency of the strains). In terms of suspension systems, the amount of large and small strains will affect the nucleation stage and crack growth stage of the rubber components. Furthermore, the damping effect on rubber fatigue can easily be seen at high strains.

Natural rubbers not only exhibit dissipative responses, or damping, at high strains, but also at small cyclic loading strains. The dissipative response is also known as hysteresis, and relationships between hysteresis and fatigue properties have been observed by many researchers [8], [12]. It has been noted that the higher the hysteresis, the lower the slope of the energy release rate. There is also an effect that occurs at the onset of the loading sequence called the Mullins effect.

Mars and Fatemi [12], [13], and [14] researched the Mullins effect, which is a phenomenon where a rapid loss in stiffness of rubber is seen after the first few loading cycles. Once the initial loss in stiffness has taken place, a steady state decline in stiffness then takes place. The result is a measurable increase in displacement with the first few successive applications of the load. Afterwards, the increase in displacement remains fairly consistent as long as the specimen does not warm up significantly. The Mullins effect varies with the magnitude of the initial loads; however, the larger the load, the larger the Mullins effect.

For this thesis, the test specimens were loaded three times before the nondestructive tests were recorded to reduce the Mullins effect. Furthermore, due to weak bonds breaking early on during the fatigue test, all test specimens were loaded 1,000 cycles before fatigue data was recorded to produce more consistent results and to reduce noise. However, this effect can still be seen after the first 1,000 loading cycles in Figure 2.1, which is a graph taken from a rubber sample that was cyclically loaded from 0-15,000 lbf. As seen in the figure, there is a sharp increase in compressive stiffness before the data levels out.

When a suspension system is loaded to its maximum capacity, an effect that often takes place within the rubber due to large strains is called strain crystallization. Harbour et al. [15] describe strain crystallization as the period when the polymer network chains become aligned such that a phase change occurs, and some of the amorphous rubber turns into a semi-crystalline material. In contrast to the Mullins effect, where the hysteresis and stiffness permanently decrease, the added stiffness and hysteresis from strain crystallization does not diminish with additional loading. In this crystalline state, rubber

exhibits an increase in resistance to crack growth. Furthermore, Fuller, et al.[16] concluded that strain crystallization is at a maximum for natural rubber around -25°C. Therefore, suspension systems that experience extreme cold will have an increase in stiffness and hysteresis. Even though this thesis will not test at different temperatures, temperature has a significant impact on the performance of the rubber components.

When rubber is subjected to repeated deformations, it can become so hot that it explodes [17], [18], [19]. This phenomenon is called "blowout." Blowout occurs when the internal heat generation becomes greater than the rate of heat dissipation into the surroundings. Damping within the rubber converts the mechanical energy into thermal energy. Because rubber is a thermal insulator, it does not conduct heat well. Therefore, the internal temperature becomes high enough to cause decomposition of the rubber component. This buildup of heat results in a rise in pressure, thus causing the component to literally explode. Through experiments presented in Gent et al. [20], the actual internal temperature of the rubber at which blowout occurred was about 200°C. Blowout may occur in the field in suspension systems that are overloaded while on a road that is extremely rough or bumpy. Excitations may be large enough to heat the rubber until it fails. Furthermore, even though heat build-up within the rubber may not cause it to explode, the heat build-up will accelerate the failure of the component. Blowout will not be addressed in this thesis because the dynamic testing frequency will be low enough to allow heat to dissipate from the component, not causing it to heat up significantly. In addition, many accelerated rubber fatigue tests (such as the ones in this thesis) require the use of a fan that blows air over the surface of the rubber products [20]. The fan helps

control the temperature of the test sample, and allows for a fatigue failure to be caused by inherent rubber failure rather than heat buildup.

2.4 Failure Criteria

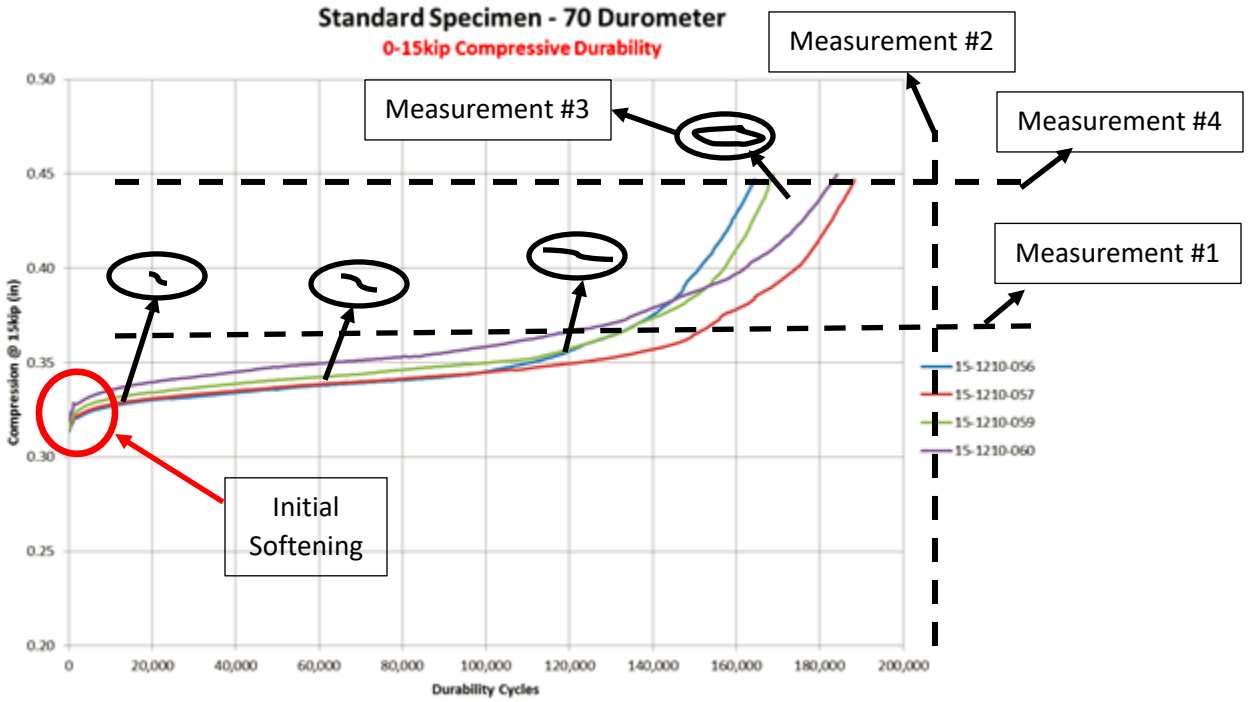

Figure 2.1: Displacement vs. Durability Cycles

In order to determine when a rubber component fails, researchers have developed several different failure measures. These measures are values that, while testing, if a limit is reached, the part is deemed to have failed. Harbour, et al. [15] created a stiffness approach that defines failure when the displacement amplitude reaches an increase of 15% of the respective initial amplitude. Measurement #1 in Figure 2.1 shows that the component would fail when the displacement increases 15% from initial displacement at

the first loading sequence. In Figure 2.1, it took 15,000lbf to compress the component 0.32 inches. According to the graph, the component might be considered failed at around 130,000 cycles where the component is compressed to 0.368 inches with the same load.

Another measure to determine failure is the number of cycles until complete rupture of the material. This method is shown as Measurement #2 in Figure 2.1. This failure measure is not ideal because it is very time consuming to run the test until complete failure; therefore, this failure method is rarely seen in literature.

Another method would be to measure the cracks within the rubber. In an experiment conducted by Mars, et al. [21], an external crack size failure criterion is used. This failure measure uses imaging technology to track the size of an *external* crack, and the component fails once the crack reaches a certain length. This failure criterion is shown in Figure 2.1 as Measurement #3, which tracks the crack length with each durability cycle. Unfortunately, crack size failure varies with the size of the rubber component. As rubber components for suspension systems are relatively large, using crack size failure is not an ideal failure criterion because crack size failure on larger objects would require very expensive testing equipment.

For this thesis, the failure measure utilized is a 40% loss in stiffness, or a 40% increase in displacement in a load-controlled test. This failure measure is not often seen in the literature, but has been used in the heavy-duty suspension system industry. This failure measure is Measurement #4 in Figure 2.1. Measurement #4 shows when the components reaches 0.448 inches of compression, which correlates to a 40% increase in compressive displacement at a 15,000lbf load. This criterion was chosen because suspension systems typically cycle from unloaded to max load (0lbf to 15,000lbf).

Therefore, this test is similar to what the rubber components might experience in the field. The 40% loss in stiffness is intended to correlate well with a vehicle situation where the operator would notice a difference in suspension performance. This could be large, visible cracks, change in shape, or change in performance.

2.5 Mechanical Load History

Once the rubber has been formulated and processed, the way it is loaded and strained will affect the fatigue life of the rubber, as well as the overall properties of it. Figure 2.2 shows the different types of loading that rubber may experience. These types of loading have been researched in [12], [15], [20], [22], [23], [24], and [25].

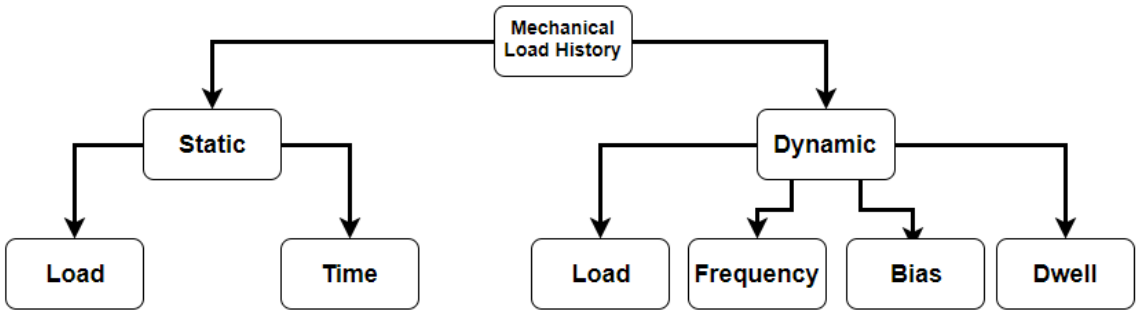

Figure 2.2: Flow Chart of Mechanical Load History

The primary consideration of mechanical load history is whether the loading is done statically or dynamically. Static loads are non-moving or non-cyclic loads. On the other hand, dynamic loading occurs when there is a varying load, or a cyclic load.

Under a static load, annealing occurs when a specimen is subjected to a load for a prolonged period of time. Annealing is when the polymer chains become aligned, but

also stretched; product shape may begin to change. This change in shape is called creep. In addition, any permanent change in shape (once the load is removed) is called permanent set. As seen in [12], annealing increases the modulus of elasticity of rubber, but decreases the fatigue life. Through experiments conducted in [12], an annealing strain (static strain) of 15% displacement produced minimum life. Therefore, components that are statically loaded for long periods of time will have a decreased life based on all the measures mentioned above. Unfortunately, suspension systems may experience high loading for extended periods of time.

The main focus of this work is to determine the characteristics and behavior of rubber under high load, high cycle dynamic loading because this is where fatigue failure typically occurs in suspension systems. The four sections of dynamic loading are frequency of the load, magnitude of the load, dwell time, and bias (R ratio) as shown in Figure 2.3.

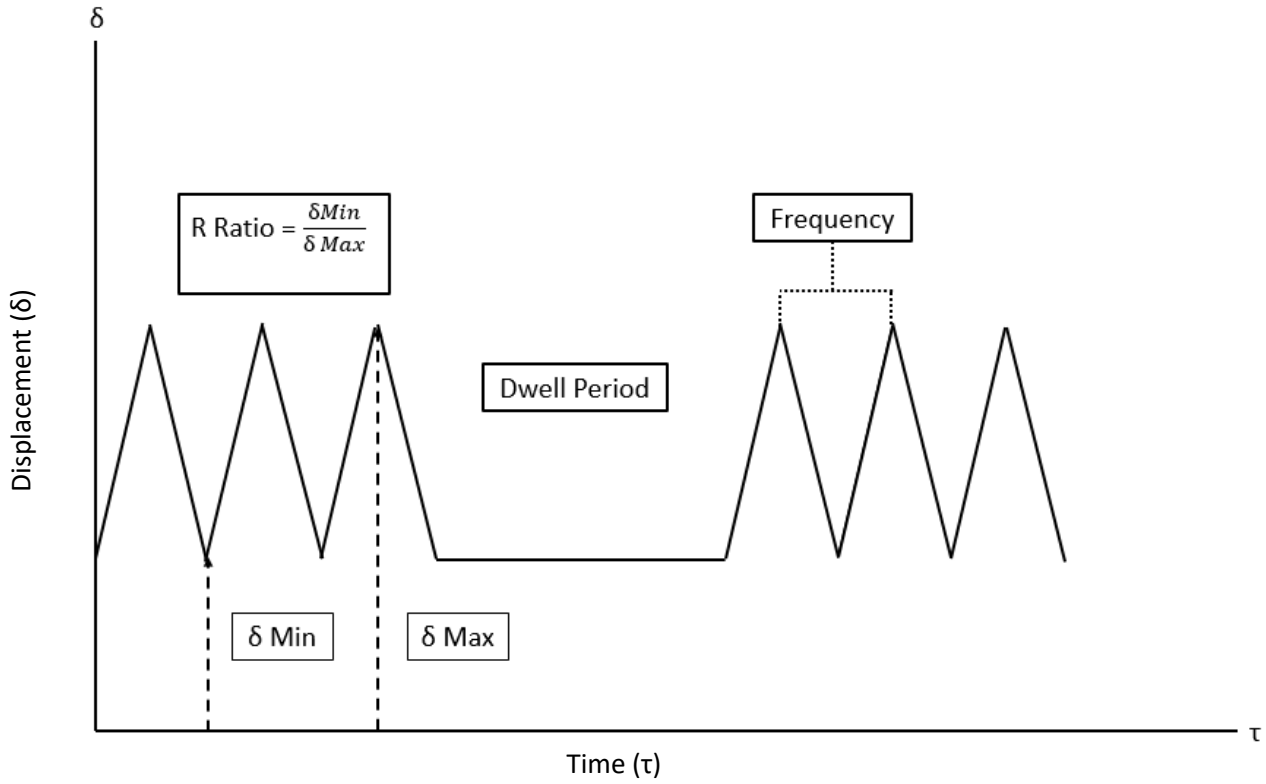

Figure 2.3: Diagram of Dynamic Loading

Rubber's fatigue behavior is very sensitive to both the maximum and minimum loads, whether it be negative (compression) or positive (tension). Mars and Fatemi [1] used a measure of the loading, called the R ratio, or bias, which is the ratio of the minimum displacement over the maximum displacement. When the R ratio is zero (if the component was fully unloaded) the fatigue life drastically decreased [24], [26], [27]. For this work, the R ratio will be zero because some of the rubber components are completely unloaded in certain operating conditions, and an R ratio of zero helps to accelerate the bench testing [24].

Mars et al. [25], studied the consequences of a dwell period between loading cycles. A relationship between crack growth rate and dwell time was experimentally

determined. It was concluded that the crack growth rate increases rapidly when the dwell period is between 0-2 seconds. The growth rate still increases as the dwell period increases, but not as drastically. Furthermore, the number of loading cycles between a dwell period plays a major role as well. An inverse relationship develops, which states that an increase in the number of loading cycles between a dwell period decreases the crack growth rate.

In addition to the number of cycles a rubber component is loaded, the frequency of these loads has also been studied. Mars and Fatemi [12] stated that the frequency of the load does not affect the fatigue life of the rubber at low frequencies (i.e. a 5Hz load and a 2Hz load will result in the same number of loads until failure). However, as the frequency of the load increases, heat can build up within the rubber component. This build up in heat can result in blowout. For this thesis, the frequency of the load will be small enough (1.5Hz) where blowout will not occur.

2.6 Environmental Conditions

Environmental conditions play a major role in the fatigue life of rubber. Both the stress-strain behavior and the fatigue properties change with varying temperatures due to specific volume and the presence and concentrations of certain chemical reactants. The suspension systems being studied are sent all over the world; therefore, the environmental conditions encountered vary greatly.

Compared to a vacuum, exposure to oxygen on the surface decreases the mechanical fatigue crack growth threshold. In addition, oxygen may dissolve in the rubber, thus inducing chemical changes to the bulk elastomer network. This process is called oxidative aging. Lindley [26] explains that due to stress concentrations, elastomer

networks at the crack tip are predisposed to react with oxygen. The oxygen reacts with the carbon-carbon bonds, causing scission. The degree of scission in the network chain depends on the presence of antiozonants and antioxidants in the rubber compound.

2.7 Creep Rate

When rubber is subjected to a static load, increasing deformation occurs, known as creep [28]. Creep is a time dependent deformation of a material when a load is applied to it below the materials yield strength. For example, if a brick is placed on a rubber mat, the mat will slowly compress over time, leaving an imprint of the brick.

There are three stages of creep: initial, second, and third, as seen in Figure 2.4. During the initial creep stage, the creep rate increases rapidly until it levels out into the second stage, where a constant creep rate is seen. Once a transition point is reached, the creep rate increases until ultimate failure of the part [29].

Creep is expressed as a percentage of total deformation minus initial deformation, divided by initial deformation. The value of creep is determined at an arbitrary time interval, such as minutes, hours, or even days.

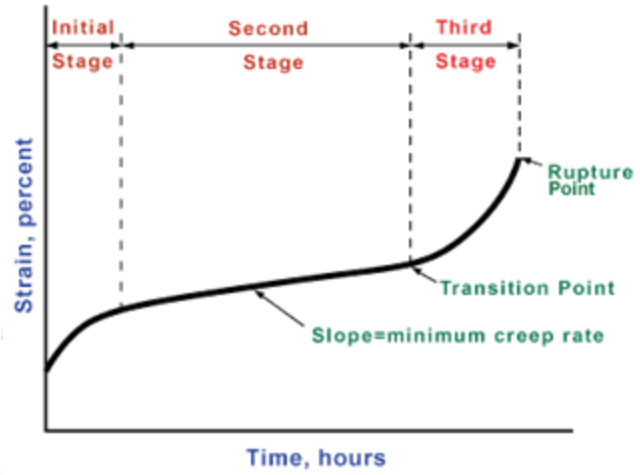

Figure 2.4: Classic Creep Rate Curve, Adapted from [29]

Even though this thesis deals with dynamic, cyclic loading, the creep rate principals can be applied. During the fatigue test of the samples in this thesis, as seen in Figure 2.1, the increase in compression versus number of fatigue cycles curve resembles a creep rate curve. Furthermore, plotting increase in compression versus the logarithmic number of fatigue cycles will allow for determination of the steady state creep rate.

2.8 Summary

The literature referenced above was used to drive the work of this thesis. Many of the aspects were used to determine the design of experiments, with some taking more consideration than others. Vulcanization is the main consideration of rubber formulation. The cure temperature and cure time will be optimized to achieve fatigue life. Mechanical behavior explains the nucleation and growth of cracks within rubber, which causes it to ultimately fail. In addition, hysteresis, the Mullins effect, strain crystallization, and blowout are phenomena that contribute to the response of rubber at various stresses and strains.

To accurately measure the performance of the rubber samples, various failure criteria were considered. Ultimately, Measurement #4 is the failure criteria chosen in this thesis. To reach failure, the way the rubber is loaded and strained is very important. For this thesis, the focus is to determine the characteristics and behavior of rubber at high load, high cycle dynamic loading. In addition to the way the rubber is loaded, the environmental conditions also play a key role in the failure of rubber. Both the stress-strain behavior and fatigue properties of rubber change with varying temperature and the presence of certain chemical reactants. The rubber samples will be manufactured and tested in a well ventilated and insulated manufacturing facility. Furthermore, the ambient air temperature will be recorded regularly to ensure no significant change while testing or molding.

CHAPTER 3

DESIGN OF EXPERIMENT

The goal of this experiment is to determine how the state of cure and cure temperature of the molding process influences the fatigue life of rubber in suspension systems. Non-controlled factors like the lot of rubber, plant temperature, and whether the sample was difficult to remove from the molding press were tracked to determine whether they affected the results. Furthermore, nondestructive tests were also performed to evaluate if nondestructive test results would correlate to the destructive test results.

3.1 Experimental Scope

For this thesis, the components will be produced within a manufacturing facility in Kendallville, Indiana, which is well ventilated and insulated. In addition, the components will be tested in an ASTM certified lab environment held at 72°F with controlled humidity. The ambient air temperature during the molding process will be recorded to ensure that there is no significant change in temperature when the components are molded. Therefore, the environmental conditions for the tests should be nearly identical to have minimal impact on the study's results. Furthermore, changing the temperature of the factory floor or testing room would be out of the scope of this experiment. The focus of this thesis is on the impact of the manufacturing processes of the rubber components and not the environmental effects on the rubber components.

3.2 Experimental Set Up

The experiment was a two-factor experiment with 5 levels of cure time and 3 levels of temperature. The experiment type was chosen because it allows for enough variability between combinations of cure time and cure temperature to see a difference in the test results.

The parameters of cure time and cure temperature were chosen because those two parameters have the largest effect on rubber components based both on experience and the literature. In addition, running more than a two-factor test with a large number of levels would take much more time to mold and test the specimens.

The levels of cure time were chosen based upon engineering judgement from a team of engineers and operators involved with both the product design and product manufacturer. It was believed that cure time may be nonlinearly related to the fatigue strength, so a large number of levels (five) were utilized. Furthermore, based on past experience, parts outside of the central cure time should fail quickly.

The levels of cure temperature were chosen similar to the cure levels. It is believed that cure temperature may also be nonlinearly related to fatigue strength, but not to the level of cure time. Therefore, a spread of temperature values was desired; however, because of cost constraints, only three levels of temperature were chosen instead of five levels.

Test samples were made from virgin rubber adhesively bonded to steel plates (dimensions of the sample can be seen in Figure 3.1). The template of the samples was based upon rubber springs that suspension manufacturer uses on one of their suspension systems, as seen in Figure 3.2. This sample is a smaller version of the part produced by a

suspension manufacturer. A smaller version was used instead of the full part because of ease of use and resources available. Larger parts require more material as well as a higher capacity machine to fatigue test the parts.

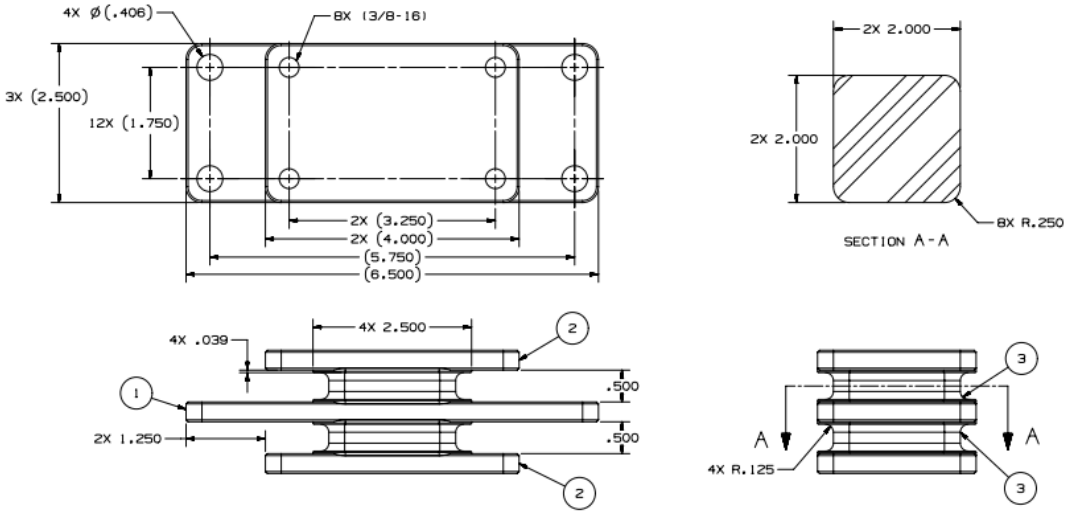

Figure 3.1: Technical Drawing of Sample

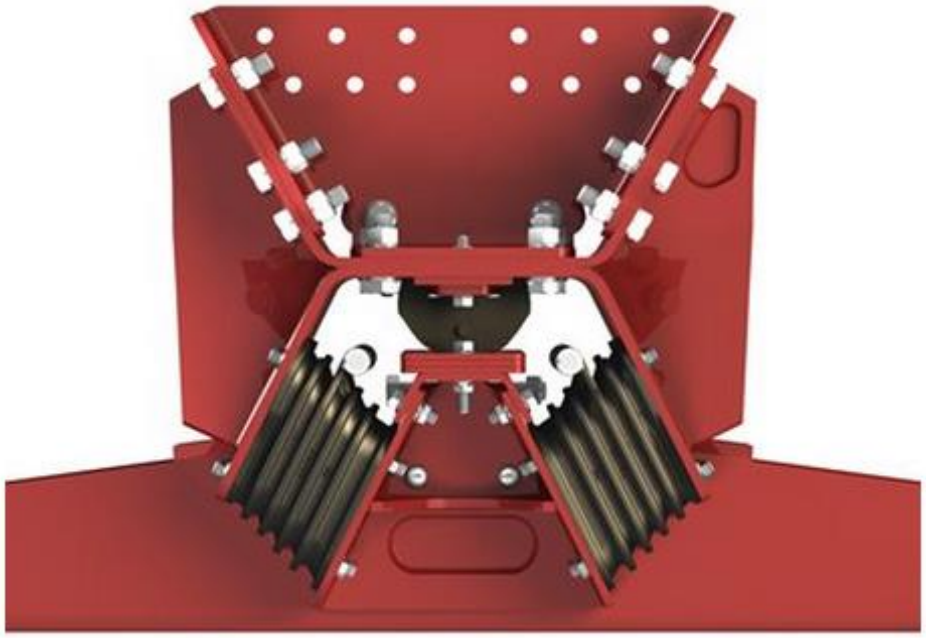

Figure 3.2: Rubber Part Utilized within a Suspension System

The particular material used in this thesis is the same material used for rubber components in a suspension system: natural virgin rubber. As there can be variation in natural rubber as it is derived from plants, samples from three different lots of material were utilized. The lots differed by production day (each 1 week apart), which entails a multitude of factors: time of year, amount of rainfall, sunlight exposure, the age of the tree at which the rubber is extracted, etc. No tests were utilized to quantify the differences in the lot of rubber as these tests are not typically performed on the incoming material.

Figure 3.3 graphically shows the experiment; each dot represents a sample made at each of the combinations. Each color represents a different lot of rubber used to mold each sample. For example, at a cure temperature at 170 degrees Celsius and a state of cure of "under (short for under cure)," 6 samples were made from each lot of rubber (i.e, 18 samples for one combination). Thus, there are 270 samples overall. To make analysis easier, from here on, under cured will be referred as state of cure 1, slightly under cure will be referred as state of cure 2, and so on. Figure 3.4 overviews the sequence of events of the experiment from start to finish.

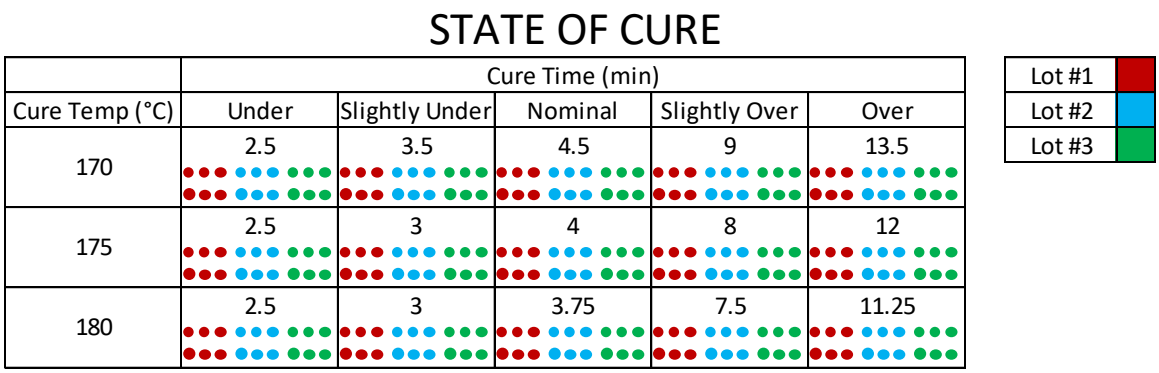

Figure 3.3: Summary of Molded Samples

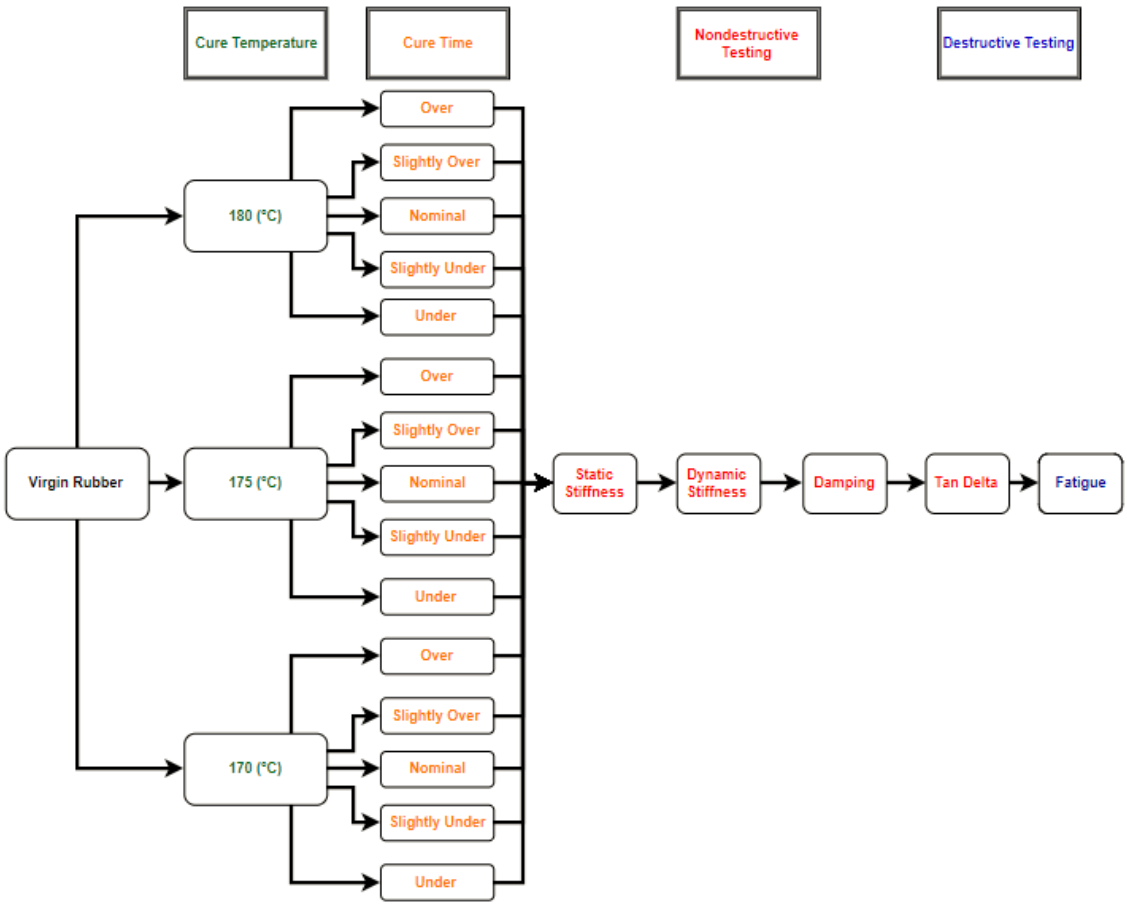

Figure 3.4: Flow Chart of Experiment

Every sample will undergo a series of nondestructive tests and destructive tests. The nondestructive tests are static stiffness, dynamic stiffness, damping, and tan delta: static stiffness is the ratio between the force applied to an object and its corresponding displacement resulting from that force, dynamics stiffness is a frequency dependent ratio between a dynamic force and its corresponding dynamic displacement, damping corresponds to the dissipation of energy from a system, and tan delta is the tangent of the phase angle between the input force wave and the output displacement wave. These tests quantify various performance aspects of the rubber. Because of the Mullins effect, each test specimen was loaded three times before any of the nondestructive tests were

performed. The nondestructive tests were performed at two frequencies (5Hz and 10Hz) to see if there was any variability between the different frequencies. The procedure to find the values of static stiffness (K_s), dynamic stiffness (K_d), damping (C), and tan delta are outlined in Appendix A. The destructive test will be the chosen fatigue test. All testing will be on one MTS-810 test machine, as seen in Figure B.1 (Appendix B) to reduce measurement error. For each specimen, the operator bolts the specimen into the MTS-810 machine.

These nondestructive test results are used to determine the rating of their suspension systems (40,000lb, 100,000lb etc. loading capacity) and to decide whether the part will meet its quality standards when out in the field. The loading capacity is the max weight of the payload the suspension can hold without failure. Therefore, the user of the truck must not load the vehicle any more than the rating given for that suspension system. Static stiffness helps dictate the loading capacity of the suspension, where damping and tan delta help dictate how smooth the drive will be.

The destructive test chosen for this thesis is rubber fatigue. Each sample will undergo cyclic loading until the failure criteria is reached (40% loss in compressive stiffness, Measurement #4 in Figure 2.1 on Page 9), and the final number of fatigue cycles will be recorded. This failure criteria was chosen based on industry experience and user input. In the automotive industry with light-duty suspension systems, a 20%-30% loss in compressive stiffness in rubber components can be noticed by the operator of the vehicle and replacement parts would be needed. In the case of this thesis (dealing with medium and heavy-duty suspension systems), it takes about a 40% loss in compressive stiffness for the operator to notice a difference in performance. Therefore, the failure

criteria of 40% loss in compressive stiffness was chosen to keep in line with industry. Also, similar to the nondestructive tests, each sample will undergo 1,000 loading cycles before data is recorded to reduce the amount of noise by breaking up the weak bonds within the rubber. During the test, the stiffness will be calculated after every 1,000 loading cycles to determine the percent loss in stiffness.

3.3 Data Analysis

The results from the nondestructive tests and the destructive test will be analyzed using a variety of statistical methods. A summary of the results example can be seen in Table B.1 (Appendix B). In addition, the nondestructive test results will be compared to the destructive test results to see if there is any correlation between them.

The results will be analyzed using three approaches: graphical, regression, and tabular. The purpose of conducting three analysis approaches is to see which one can be understood the best, and so future projects can decide which approach fits its needs.

- The graphical approach was used to visually see how the destructive and nondestructive results change due to a change in cure parameters, as well as see correlations between the nondestructive and destructive test results. This approach will utilize a main effects plot, an interval plot, and an interaction plot.
- The regression approach utilizes Minitab's regression algorithms to predict destructive and nondestructive test results based on data collected from the experiment. For example, based on data collected on fatigue throughout the experiment, an equation will be produced to predict what

the fatigue life would be if one would create another rubber sample with a certain combination of cure time and cure temperature.

- The tabular approach helps determine whether certain cure parameters have a significant effect on the destructive and nondestructive test results by giving each parameter a probability value (i.e. an ANOVA table). The probability values given, as seen in Table B.2 (Appendix B), are calculated using a student t test. Each cure parameter produces different fatigue results, and each cure parameter produces samples with a mean and standard deviation of fatigue cycles. For example, for state of cure 1, the fatigue results of all the samples tested where the state of cure is 1 are compared to all the other samples that were tested using different states of cure, regardless of the cure temperature. The null hypothesis of this student t test is that the mean values of the fatigue results should be the same, but if the p-value is less than 0.05, then the fatigue results are different. Therefore, it is statistically significant that state of cure 1 affects the fatigue results on its own.

In the case of this thesis, outliers were handled based off data results and the associated treatment of the component. The components that had very low fatigue lives were coincidently the components that had to be forced out of the mold with a hammer once the manufacturing process was complete. The part, because of poor steel insert fit and/or swelling of the rubber, was stuck in the mold after the completion of the manufacturing process, and had to be hit out. These components had significantly lower

fatigue lives than the other components with the same cure parameters; therefore, they were deemed outliers.

CHAPTER 4

STATISTICAL ANALYSIS

4.1 Introduction

The results obtained for this thesis include values of static stiffness, dynamic stiffness, damping, tan delta, and fatigue life for each of the specimens. The numbers after K_d, C, and tan delta in Table 4.1 represent the frequency at which the test was conducted. The static stiffness (K_s) test was not done dynamically, and therefore does not have a number after it. To analyze the data, Minitab is utilized; a table of data that is inserted into Minitab can be seen below in Table 4.1:

Table 4.1: View of Data in Minitab

Sample ID	Cure Temp	Cure Time	Ks	Kd5	C5	Tan5	Fatigue
001	170	2.5	23731	35631	185	0.1657	270600
002	170	2.5	23491	34848	179	0.1631	232000
003	170	2.5	23234	34230	171	0.1593	230900
004	170	2.5	11259	17342	88	0.1623	100700
007	170	3.5	22905	34582	182	0.1678	113900
008	170	3.5	24031	35856	181	0.1606	240100
010	170	3.5	23771	35395	177	0.1594	274700
013	170	4.5	24001	36263	190	0.1670	183900
014	170	4.5	24600	37019	190	0.1636	189400

Various statistical techniques were used in order to conclude which combination of state of cure and cure temperature would produce the longest fatigue life, and whether there is any correlation between any of the nondestructive test results (K_s, K_d, C, Tan Delta) and the destructive test results (fatigue).

4.2 Termination of Fatigue Testing

During the fatigue testing portion of the experiment, inconsistencies in the fatigue cycle results became apparent. Preliminary analysis was conducted as soon as sample testing was completed. As a single fatigue test lasted roughly two to three days per sample, only two to three samples could be tested during a given week. Considering the limited testing capacity along with the inconsistent results, Figure 4.1 shows the samples that were tested before the termination of the fatigue testing.

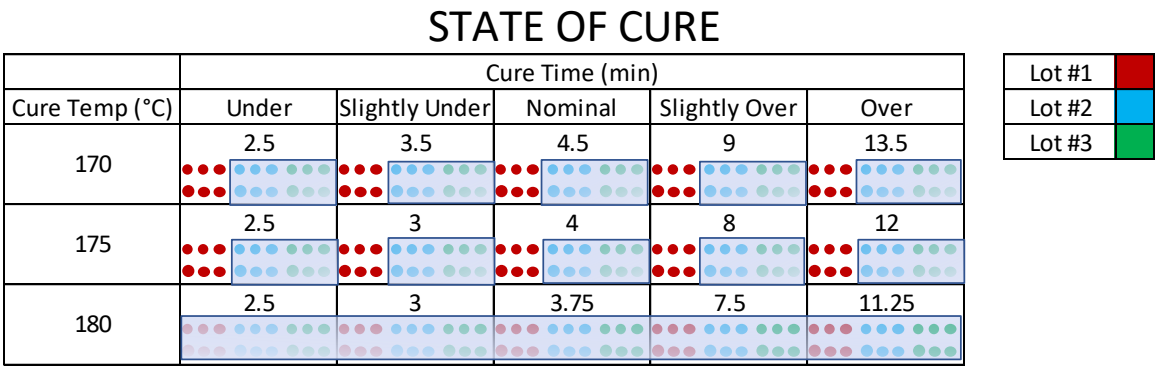

Figure 4.1: Analyzed Preliminary Testing Samples

Due to the experiment set up and the order of the testing, only one lot and two temperatures were tested. The red samples in Figure 4.1 (i.e., not blurred out) were the samples that were fatigue tested prior to the termination of the fatigue testing. As seen in the analysis below in Section 4.3, the reason for not fatigue testing the 180 degrees Celsius samples is because of the minimal variation between the cure temperatures 170 degrees Celsius and 175 degrees Celsius. In addition, lot to lot variation was to be tested once the remaining Lot #1 (i.e., the red dots) samples were fatigue tested. Because of the inconsistencies in the fatigue test, variation between the different lots would be difficult

to distinguish. Furthermore, as will be discussed below, resources were allocated to create a new sample specimen that will allow for more consistent fatigue results. However, the analysis below will be based on the nondestructive and destructive test results of the samples in Figure 4.1.

4.3 Fatigue Life

4.3.1 Graphical Approach

To determine the parameters' effect on the fatigue life, a graphical approach was performed. As depicted in Figure 4.2, an increase in the state of cure decreases the fatigue life of the samples. The state of cure numbers corresponds to "under", "slightly under" etc. with state of cure 1 being "under" cured and so forth. The change in fatigue life due to an increase in the state of cure is known as a main effect; a main effect is when all other variables are held constant (cure temperature in this case), the desired outcome (fatigue) is affected by changing a single variable (state of cure). In this experiment, when either cure temperature is chosen (170 or 175 degrees Celsius), fatigue is affected the same way by changing the state of cure up or down.

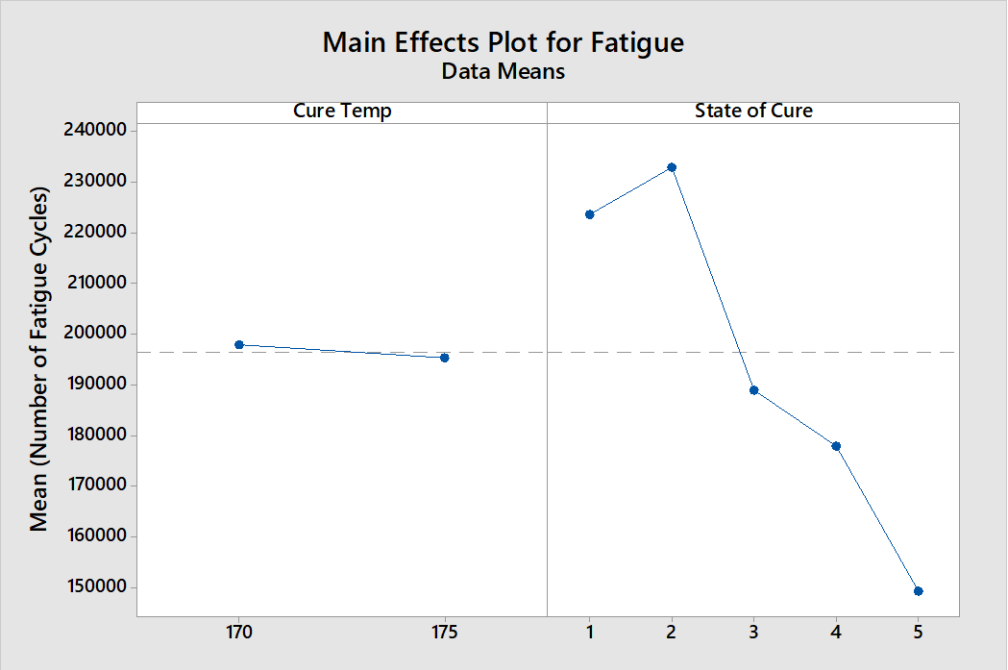

Figure 4.2: Main Effects Plot of State of Cure and Cure Temperature for Fatigue

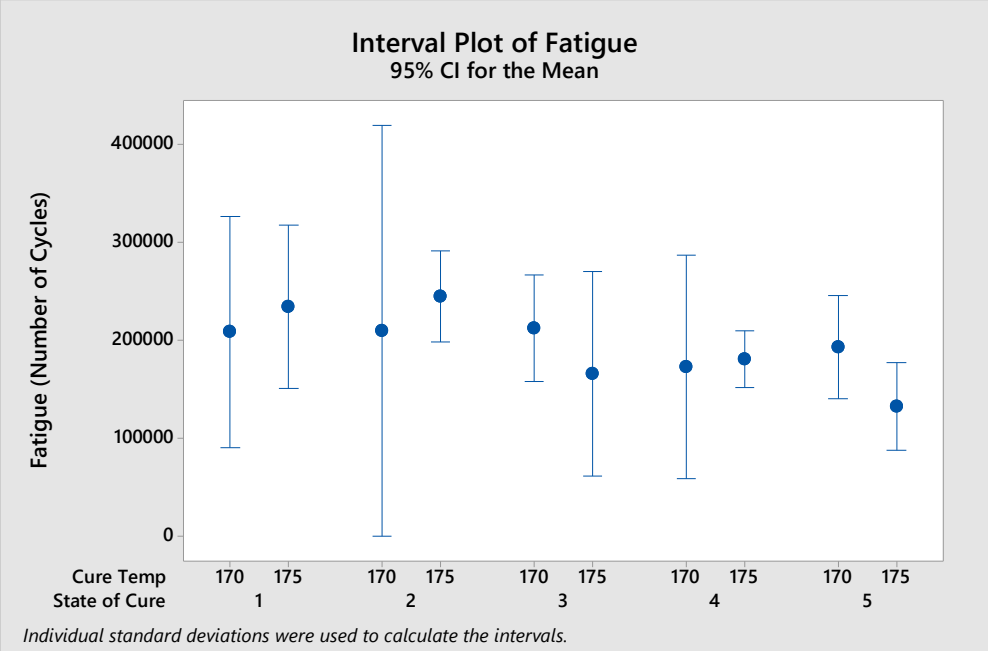

Figure 4.3: Interval Plot of State of Cure and Cure Temperature for Fatigue

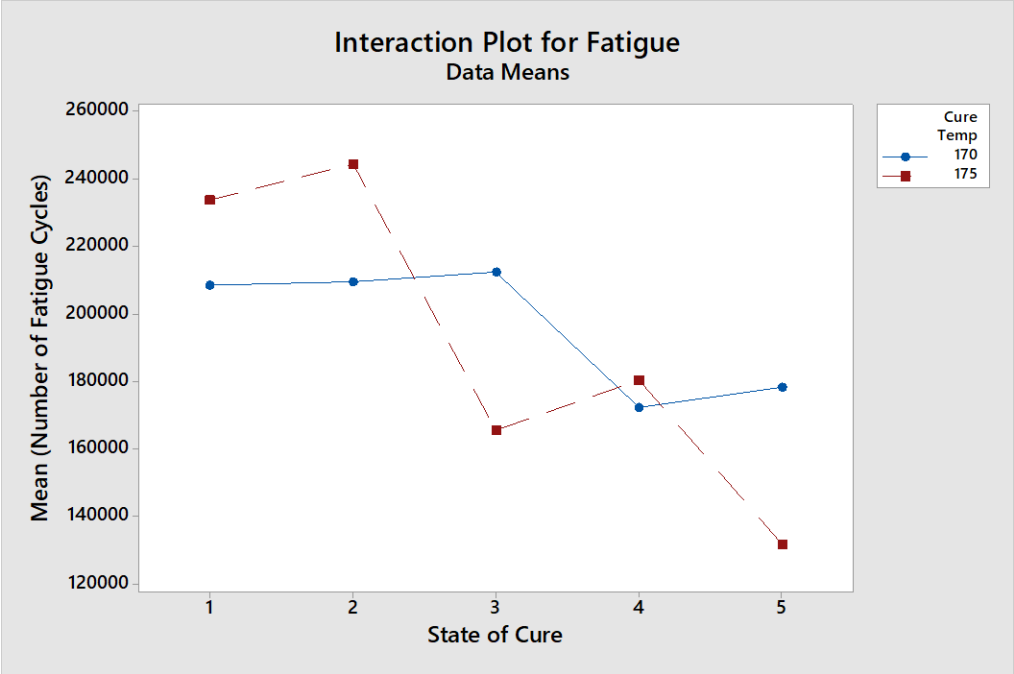

Figure 4.4: Interaction Plot of State of Cure and Cure Temperature for Fatigue

An interval plot, as seen in Figure 4.3, shows that 95% of the fatigue results are between two certain values given a certain combination of state of cure and cure temperature. An interaction plot was then formed as seen in Figure 4.4. This plot shows the fatigue life for each combination of state of cure and cure temperature. The y-axis is fatigue life, and the states of cure are depicted on the x-axis, with the different temperatures being depicted using different colored lines. Interaction effects occur when certain combinations of variables produce the same outcome (i.e, if a high temperature and low state of cure and a low temperature and high state of cure produced the same fatigue life). An interaction exhibits itself like an "X" in a plot, where the top corners of the "X" exhibit the same y-axis outcome but have a different combination of parameters. However, in terms of fatigue, there are no interaction effects because the only variable studied that seems to truly effect the fatigue life is state of cure.

4.3.2 Regression Approach

To predict the fatigue life of a sample given the state of cure and cure temperature, a regression equation was created using the general factorial regression feature in Minitab. This feature creates a regression equation that includes all the main effects and interactions with coefficients. A main effect is the state of cure and cure temperature, where interactions are specific combinations of states of cure and cure temperatures. The larger the coefficient in front of the main effect or interaction means that cure temperature or state of cure has a significant effect on fatigue life. To determine the number of fatigue cycles for a given combination of cure time and temperature, Equation 1 states:

$$\begin{aligned} Fatigue \;=\; & 195223 \;+\; 3890\; Cure\; Temp_{170} \;-\; 3890\; Cure\; Temp_{175} \\ & +\; 26002\; State\; of\; Cure_1 \;+\; 31894\; State\; of\; Cure_2 \\ & -\; 6198\; State\; of\; Cure_3 \;-\; 18665\; State\; of\; Cure_4 \\ & -\; 33033\; State\; of\; Cure_5 \;-\; 16565\; Cure\; Temp_{170} * State\; of\; Cure_1 \\ & -\; 21440\; Cure\; Temp_{170} * State\; of\; Cure_2 \\ & +\; 19535\; Cure\; Temp_{170} * State\; of\; Cure_3 \\ & -\; 7949\; Cure\; Temp_{170} * State\; of\; Cure_4 \\ & +\; 26420\; Cure\; Temp_{170} *\; State\; of\; Cure_5 \\ & +\; 16565\; Cure\; Temp_{175} * State\; of\; Cure_1 \\ & +\; 21440\; Cure\; Temp_{175} * State\; of\; Cure_2 \\ & -\; 19535\; Cure\; Temp_{175} * State\; of\; Cure_3 \\ & +\; 7949\; Cure\; Temp_{175} * State\; of\; Cure_4 \\ & -\; 26420\; Cure\; Temp_{175} * State\; of\; Cure_5 \end{aligned} \tag{1}$$

For example, to determine the predicted fatigue life for a sample with a cure temperature of 170 degrees Celsius and a state of cure of 1 (under cure), you add up the coefficients that include only "Cure $Temp_{175}$" and/or "State of $Cure_1$." (195223 + 3890 + 26002 – 16565 = 208,550). All the other factors are zero. Therefore, the main effect that has the biggest influence on fatigue life is state of cure 5 (over cure) with a coefficient of -33033. In addition, the interactions with the largest effect on fatigue life are cure

temperature of 170 degrees Celsius with state of cure 5 (over cure) and cure temperature of 175 degrees Celsius and state of cure 5 (over cure), with coefficients of 26420 and -26420, respectively. It is rare to have the same magnitude of coefficients. Additional information can be gathered from this equation by comparing the main coefficients of the main effects. As seen in the equation, fatigue is increased with a cure temperature of 170 degrees Celsius and a state of cure of either 1 (under cure) or 2 (slightly under cure).

Figure B.2 (Appendix B) shows that the regression equation above does not fit the actual fatigue data very well due to the variation seen in the fatigue testing. Having high residuals means that the predicted fatigue from the equation above and the actual fatigue results from testing do not match. A residual of 100,000 means that the predicted value from the regression equation and the observed value from the actual fatigue testing differ by 100,000. For example, if the regression equation predicts that the fatigue life for a certain combination of cure time and cure temperature should last 200,000 cycles and the actual sample only lasts 100,000 cycles, the residual is 100,000 (200,000-100,000 = 100,00). The top left graph of Figure B.2 (Appendix B) shows the percentage of fitted values that have a residual lower than the indicated x-value. For example, 10% of the fitted values will have a residual lower than -95,000. The bottom left histogram shows the frequency at which the indicated residual is seen. The top right “versus fit” graph shows the residuals at each fitted value. Because there are multiple samples tested at each combination of cure time and state of cure, there are multiple residuals at each fitted value. Finally, the lower right graph lists the samples in order and shows each of their corresponding residual values. There is no pattern to the residuals; therefore, the regression equation created is the best possible equation because the residuals seem to be

random. If the residuals had a pattern, then the regression equation could be tweaked to create a better prediction of fatigue life.

4.3.3 Tabular Approach

As it is difficult to determine significance of the parameters in the regression equation due to the differing units used, Minitab provides a probability value (i.e. p-value) to help determine if the main effects and the interactions have a statistically significant effect on fatigue. To conclude if a main effect or interaction influences fatigue, the p-value is compared to a significance value. If the p-value is less than 0.05, then that interaction or main effect has a significant effect on fatigue. In Table B.2 (Appendix B), the p-value of each of the coefficients in the fatigue equation are presented. The lowest p-values out of all the main effects and interaction effects are 0.075 and 0.072 for state of cure 2 (slightly under cure) and state of cure 5 (over cure), respectively. Thus, the main effects are not statistically significant, but are close. This result is also corroborated by the regression equation where states of cure 2 (slightly under cure) and 5 (over cure) have the largest coefficients. Furthermore, as seen in Figure 4.2, the state of cure that produces the largest number of fatigue cycles is state of cure 2 (slightly under cure), and the state of cure that produces the lowest number of fatigue cycles is state of cure 5 (over cure).

4.4 Nondestructive Test Results

Please see Appendix A for all nondestructive test results and analysis.

4.5 Correlation between Nondestructive and Destructive Tests

A secondary objective for this study is to provide a way to predict the fatigue life of components by testing the components in a nondestructive manner (i.e, testing the static stiffness to predict the fatigue life). The primary way used in this thesis to determine if the nondestructive test parameters could predict the components fatigue life was by using the graphical approach.

The scatter plots shown in Figures B.14-B.17 (Appendix B) exhibits how the fatigue data is correlated to each of the nondestructive test results for each sample. Each point on the graph represents a sample, and their corresponding fatigue life and nondestructive test parameter are plotted. As seen in Figures B.14 and B.15 (Appendix B), there is a slight increase in fatigue life when the static stiffness and dynamic stiffness increases, however; due to inconsistency and irregularity of the fatigue data, there is not conclusive evidence to state that there is a statistically significant correlation between fatigue and static stiffness. There seems to be no correlation between fatigue and damping, as seen in Figure B.16 (Appendix B). Finally, there is a slight decrease in fatigue when tan delta increases, but again, due to the inconsistency of the fatigue results, there is not conclusive evidence of this correlation.

4.6 Discussion

4.6.1 Discussion on Results

These test results suggest fatigue is maximized with a cure temperature of 175 degrees Celsius and a state of cure of 2 (slightly under). However, due to the variability in the test results, this conclusion is less definitive. Also note that when the state of cure

exceeds 3 (nominal cure), fatigue drastically decreases independent of the cure temperature. Therefore, it is better to under cure the rubber component rather than over-cure it.

Similar to the literature reviewed, compressive stiffness values during this testing rapidly declined during the initial loading cycles (Figure 2.1). Compressive stiffness then slowly decreased until the failure criteria of 40% loss in compressive stiffness was achieved. In addition, even though the frequency of the fatigue test was relatively low (1.5Hz), a fan was utilized to keep the temperature of the component from rising enough to "blowout." The use of the fan minimized heat build-up and helped create more consistent fatigue results.

Static stiffness is maximized at a state of cure of 3 (nominal cure) regardless of the cure temperature. When graphing static stiffness versus state of cure and cure temperature, as seen in Figure B.3 (Appendix B), a negative parabolic-like shape with a local maximum at state of cure 3 (nominal cure) is seen. Similar results are seen for dynamic stiffness and damping. Lastly, tan delta increases with an increase in state of cure regardless of cure temperature, as seen in Figure B.9 (Appendix B). In terms of rubber analysis for suspension system components, there is not much information on tan delta.

Based on the results from this experiment, it is inconclusive whether any of the nondestructive results correlate to the destructive test. However, it is possible to predict nondestructive test results based on the experimental results (i.e., it is possible to predict which parameters affect the nondestructive measures the most). The graphical, regression, and tabular approaches used in this thesis paint a similar picture of analysis in

terms of consistent results (analysis from each approach results in the same conclusions). However, some test specimens had to be forcibly removed from the mold. These samples performed very poorly in the fatigue test, and ultimately were thrown out of the analysis as outliers.

When trying to correlate the nondestructive test results to the destructive test results, the data produced does not give any clear conclusions. The literature states that the higher the damping (hysteresis), the lower the slope of the energy release, which correlates to a higher fatigue life. This correlation between higher damping and fatigue cannot be seen due to the inconsistencies of the fatigue results; therefore, this experiment does not allow for correlation between nondestructive and destructive test results.

Even though many of the noise factors were accounted for when the rubber samples were created, (same molding machine, same processor, same testing temperature etc.) rubber always has microscopic flaws when the molding process is finished. Furthermore, these microscopic flaws occur in random spots on the sample, thus propagating cracks in different areas from sample to sample. Different crack locations affect the fatigue life because some cracks can propagate faster than others depending on their location. Also, because the rubber was being fatigued over the bond line (i.e., the rubber was bulging over steel plates) during the fatigue test, the location of those microcracks became a major issue. If one of those microcracks were located where the rubber folds over the steel plates, the propagation of those cracks is expedited. In addition to the rubber being cut by the edges of the plates, there may also be stress concentrations near the microcracks as well as the microcracks being near the adhesive that bonds the

rubber to the steel plates. Either of these innocuous flaws can cause inconsistencies in the fatigue results.

4.6.2 Discussion on Improved Test

Because the rubber was folding over the steel plates which caused the rubber to be cut, a new fatigue test was designed to combat this issue. Rather than laying the coupon flat and testing in compression, the coupon was turned vertically, and a shear test was performed. A shear test was chosen because the rubber would not be overlapping the steel plates in this motion direction. Therefore, a rubber material failure would most likely be seen rather than a rubber failure due to being cut over the steel plates. The setup for this test can be seen in Figure 4.3.

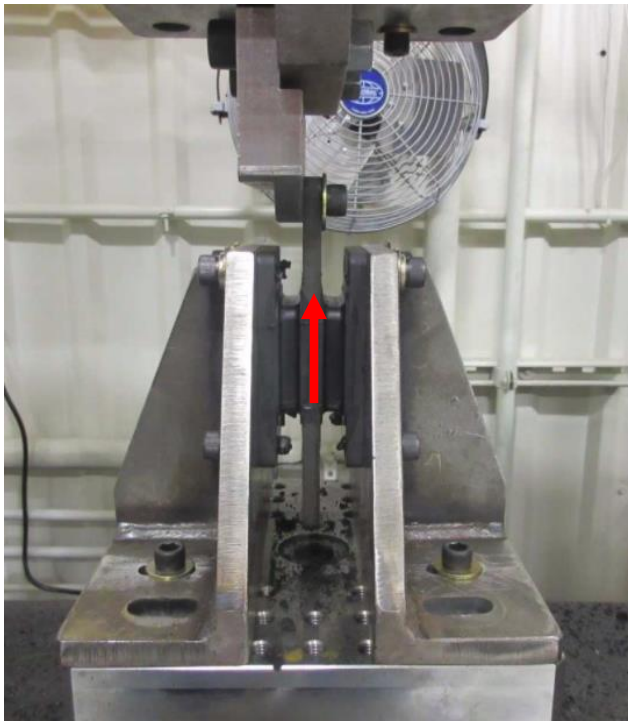

Figure 4.3: Vertical Shear Test

However, while attempting to create a test with the right amplitude and frequency, the coupons typically failed at the bond line rather than in the body of the rubber. The bond line is where the rubber meets the steel, and an adhesive (acts like glue) is used to bond the two materials together. The coupons tested with various amplitudes and frequencies all tore at the bond line first. Therefore, this fatigue test setup does not solve the issue of the fatigue test variability because ultimately the rubber must fail first, thus showing a difference in rubber quality rather than adhesive quality.

4.7 Secondary Design of Experiment

Because of the inconsistencies in the fatigue results with the sample specimen chosen for the original design of experiment, an improved sample specimen was created. Although the original design of experiment did not yield consistent fatigue results, a secondary design of the experiment with an improved sample specimen could produce insightful results. The new sample specimen was designed so that rubber should not roll over the plate edges while compressed. The sample specimen contains two outer steel plates and an hourglass rubber section between them (Figure 4.4) manufactured using the same process as the original sample specimen. Rather than a compression fatigue test, the nondestructive test for these sample specimens will be fatigue due to tension.

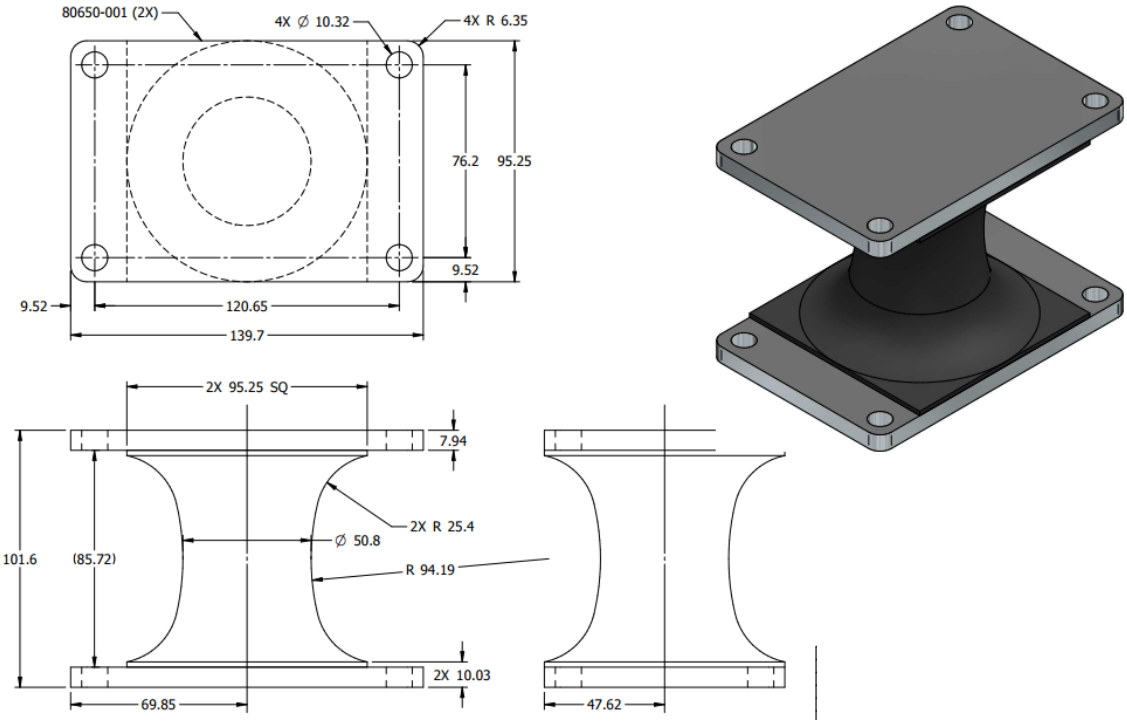

Figure 4.4: Improved Sample Specimen Design

The design utilized were based upon other research and learnings from the original experiment. Many previous studies [1, 2, 6, 8] have used a tension fatigue test to characterize rubber. Furthermore, the hourglass shape was chosen based on previous studies as well as key points in this thesis. The hourglass shape allows the sample to fail due to rubber strain, rather than being sliced over the end of the steel plate during a compression test.

To vet the design, several sample specimens were analyzed using finite element analysis software to determine where the sample specimen would crease when compressed. It is easier to determine if the shape of the sample specimen is uniform by testing it in compression rather than in tension. The FEA was run using a displacement-controlled test, where one plate of the sample specimen was fixed, and the other plate was moved a specified distance. In order to produce data that is hopefully discernable

between combinations of cure parameters, the sample specimen should crease exactly in the middle. If the coupon folds over at various spots or has multiple creases, the fatigue results will be inconsistent because those extra creases and folds may cause the sample specimen to buckle in various locations. For example, in Figure 4.5, the sample specimen has multiple creases (black arrows are pointing to the creases), which will ultimately skew the fatigue results. On the other hand, as seen in Figure 4.6, that sample specimen only creases in the middle of the rubber section. Therefore, the coupon in Figure 4.6 was pursued because it was believed to produce the most consistent results.

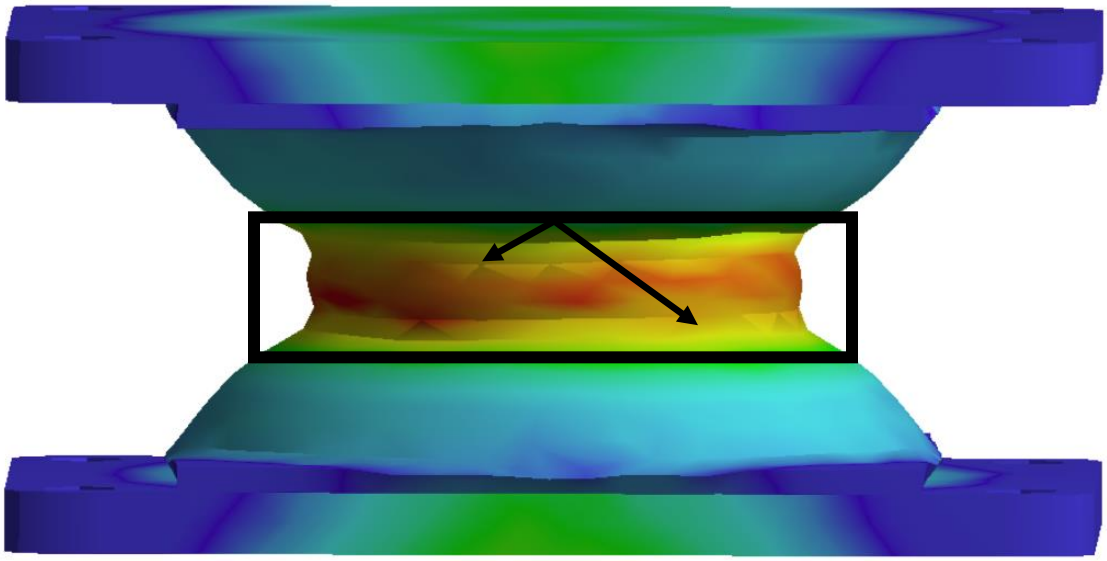

Figure 4.5: FEA of a Coupon that Contains Multiple Creases

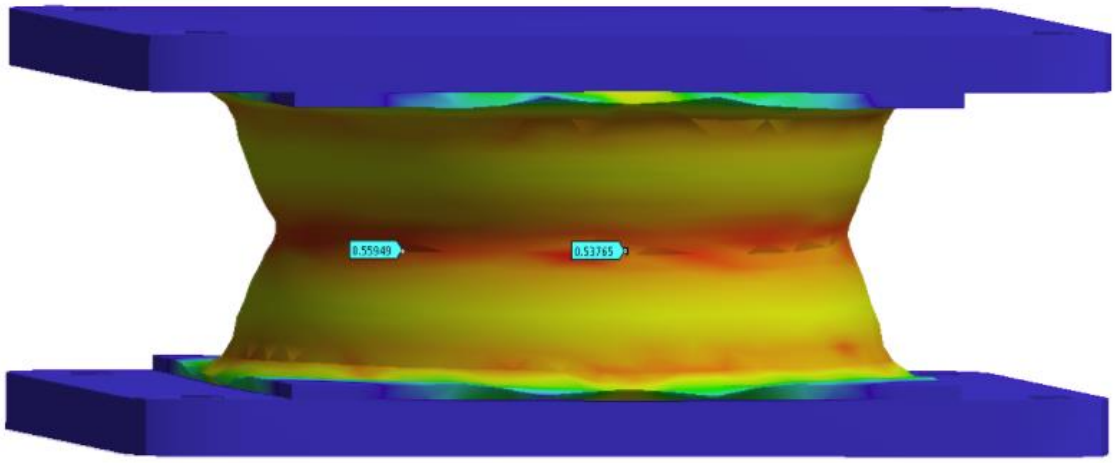

Figure 4.6: FEA of a Sample that Contains One Crease

4.7.1 Experimental Setup

A new design of experiment was created with the new sample specimen. This design of experiment is similar to the original design. The main differences are: 3 samples per combination of cure time and temperature rather than 6, three combinations of cure time and temperature (compared to 15 combinations in the original design of experiment), and 1 lot of rubber. Even though lot to lot variation was not studied in the original design of experiment, knowledge gained through running the experiment shows that variation between lots of rubber that were produced so close together (one week) would not be statistically significant due to the noise in the fatigue test.

A summary of the samples molded is shown in Figure 4.7. The cure temperature used for the new design of experiment is 175 degrees Celsius, and the three cure times are 6 minutes, 9 minutes, and 20 minutes. The “CC” next to the 6 minutes stands for “crash cooled,” where the sample specimens were placed in room temperature water for one hour after they were molded. The reason to cool the samples was to keep the internal rubber from continuing to cure after the specimen was taken out of the mold.

STATE OF CURE			
	Cure Time (min)		
Cure Temp (°C)	Under	Nominal	Over
175	6 (CC)	9	20

Figure 4.7: Summary of Molded Samples

As previously stated, the new sample specimens were tested in tension rather than compression. That means that all the nondestructive and destructive tests will be performed in tension. The nondestructive tests will be performed at the same frequency as the original sample specimens (5Hz). The fatigue test will be a tension test from 0lbf to 900lbf at 1.5Hz. These test parameters were chosen based on preliminary fatigue test development, resulting in a fatigue test that was neither too aggressive nor too lax. The fatigue test was run until the specimen completely separates into two pieces. A fan blowing on the specimen during the fatigue test was used to ensure blowout did not occur. Figure 4.8 depicts the flow of the new experiment.

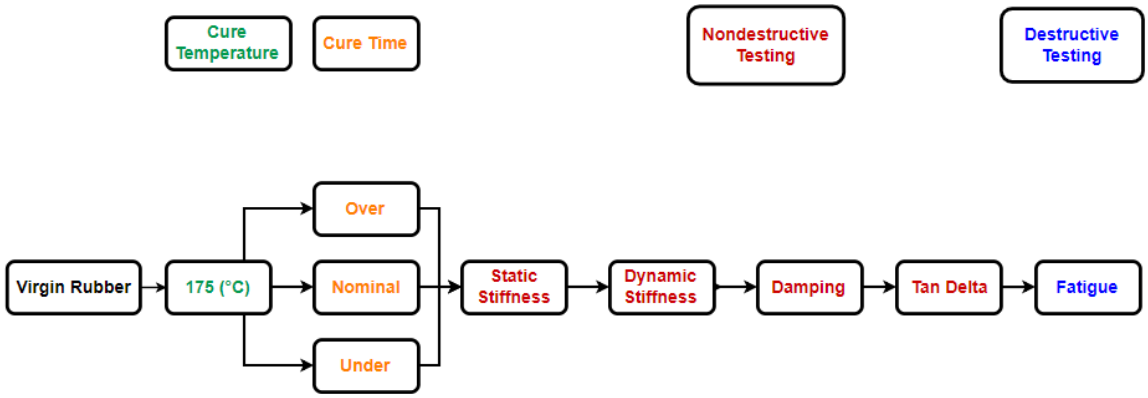

Figure 4.8: Flow Chart of Experiment

4.7.2 Results and Discussion

A summary of the results can be seen in Table 4.2. It should be noted that for the cure time of 6 minutes, the sample specimens were “crashed cooled” for one hour in room temperature water after they were removed from the mold. Also, the nondestructive tests of dynamic stiffness, damping, and tan delta were performed at 5 Hertz.

Table 4.2: Results of Secondary Design of Experiment

Sample ID	Cure Temp (C)	Cure Time (Min)	Ks (lbf/in)	Kd (lbf/in)	C (lbf*s/in)	Tan (unitless)	Fatigue Cycles
0	175	6	1205	5439.90	25.884	0.1512	403068
3	175	6	1352	5057.59	26.745	0.1685	532010
4	175	6	1275	5218.15	25.900	0.1580	450814
25	175	9	1129	5215.86	24.350	0.1483	130921
27	175	9	1185	5375.18	24.911	0.1472	348199
28	175	9	1185	5342.04	24.620	0.1464	543614
56	175	20	1030	4904.63	23.580	0.1528	212766
57	175	20	1021	4859.47	23.479	0.1540	203819
58	175	20	1033	4866.42	23.350	0.1525	324828

The focus for this experiment is to see if there is any correlation between the fatigue life of a sample specimen and its corresponding cure parameters, as well as any correlation between fatigue life and nondestructive test results. Furthermore, the new sample specimen design was used to see if more consistent fatigue life results could be obtained. From what was learned during the original design of the experiment, the analysis shown for this experiment will only include the graphical approach.

Because there is only one cure temperature for this experiment, an interval plot and main effects plot for fatigue versus cure time were produced. As seen in Figures 4.8 and 4.9, fatigue life seems to decrease with an increase in cure time. However, with a

large variation for samples tested with a cure time of 9 minutes (as seen in Figure 4.8), that correlation is not definitive.

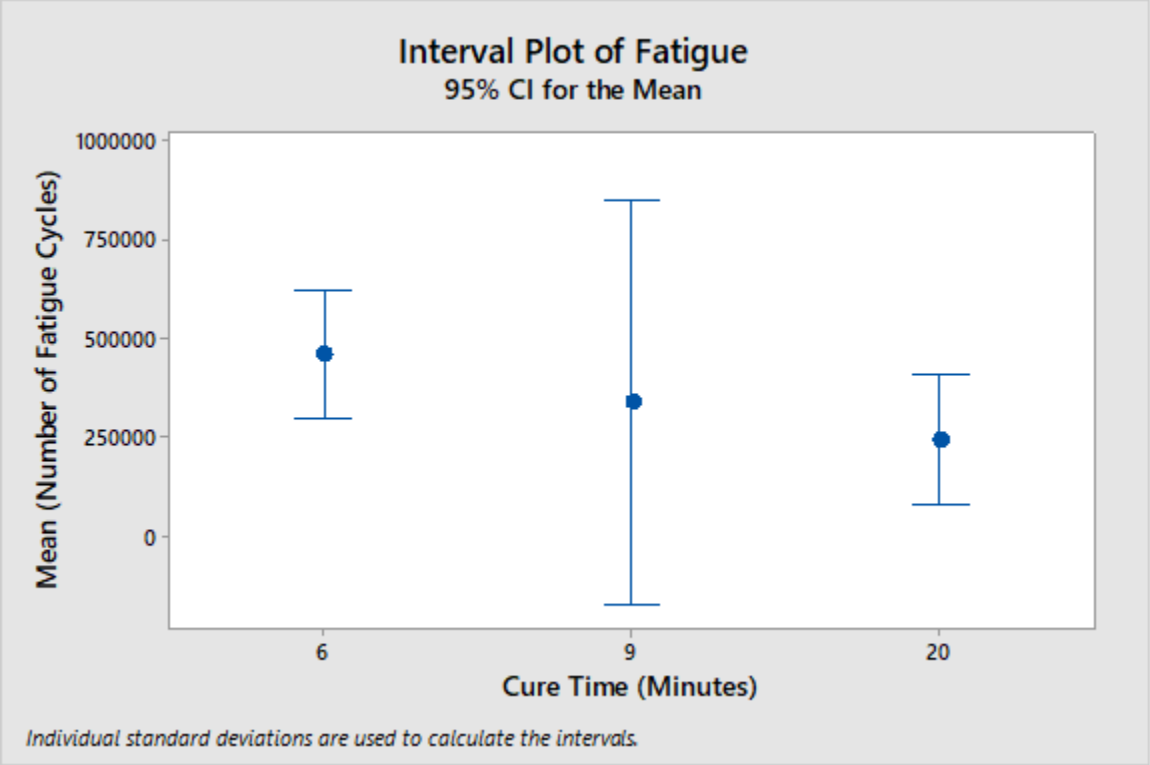

Figure 4.8: Interval Plot of Cure Time for Fatigue

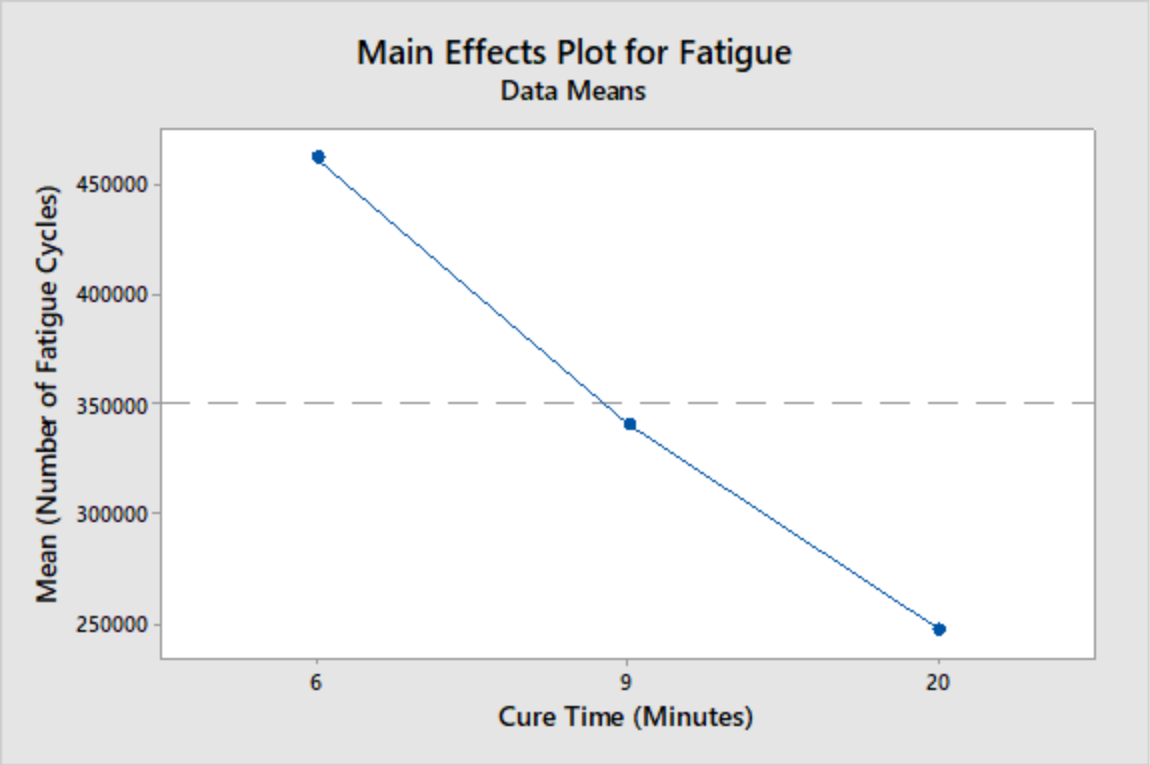

Figure 4.9: Main Effect Plot of Cure Time for Fatigue

Fatigue life was compared to the four nondestructive tests (see Figures 4.10 to 4.13). As seen in Figure 4.10, an increase in static stiffness seems to be linear compared to fatigue life (minus the outlier). Dynamic stiffness and fatigue have a lesser linear correlation when comparing fatigue life and static stiffness. There does seem to be an increase in fatigue life with an increase in dynamic stiffness, but it is not definitive (Figure 4.11). In addition, the damping versus fatigue life plot follow the same line of thought as the dynamic stiffness versus fatigue life plot: there is a linear correlation between damping and fatigue life, but it is not definitive (Figure 4.12). Finally, there seems to be no correlation between fatigue life and tan delta, as seen in Figure 4.13.

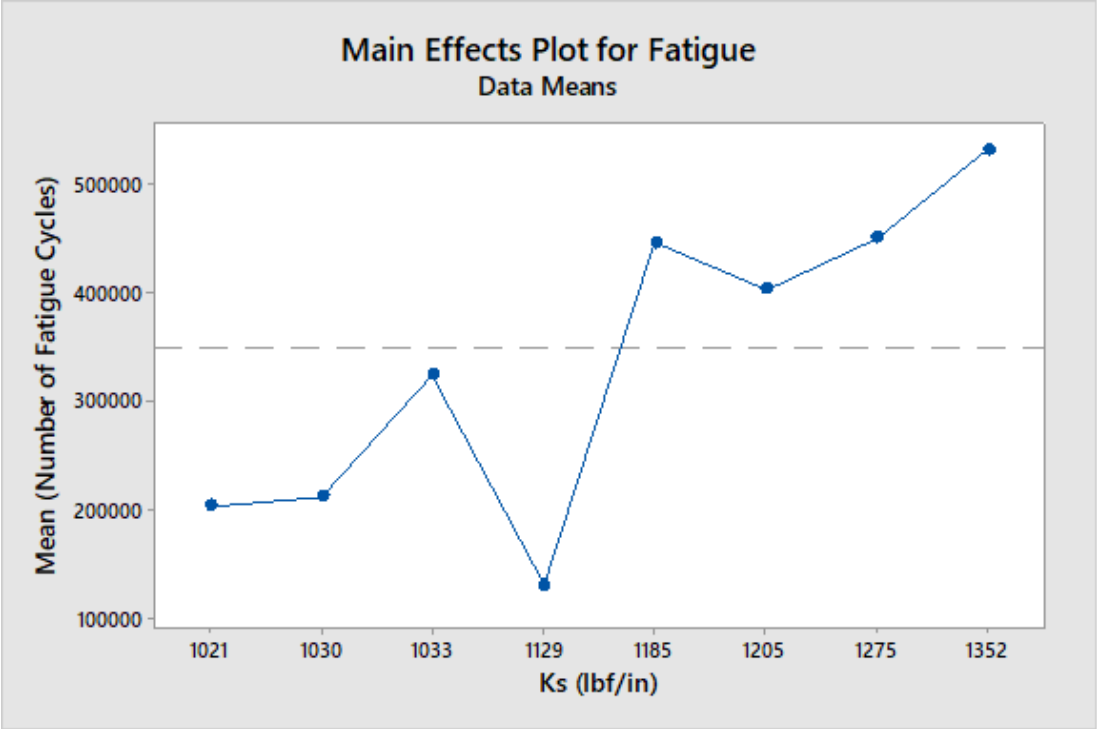

Figure 4.10: Fatigue Versus Static Stiffness

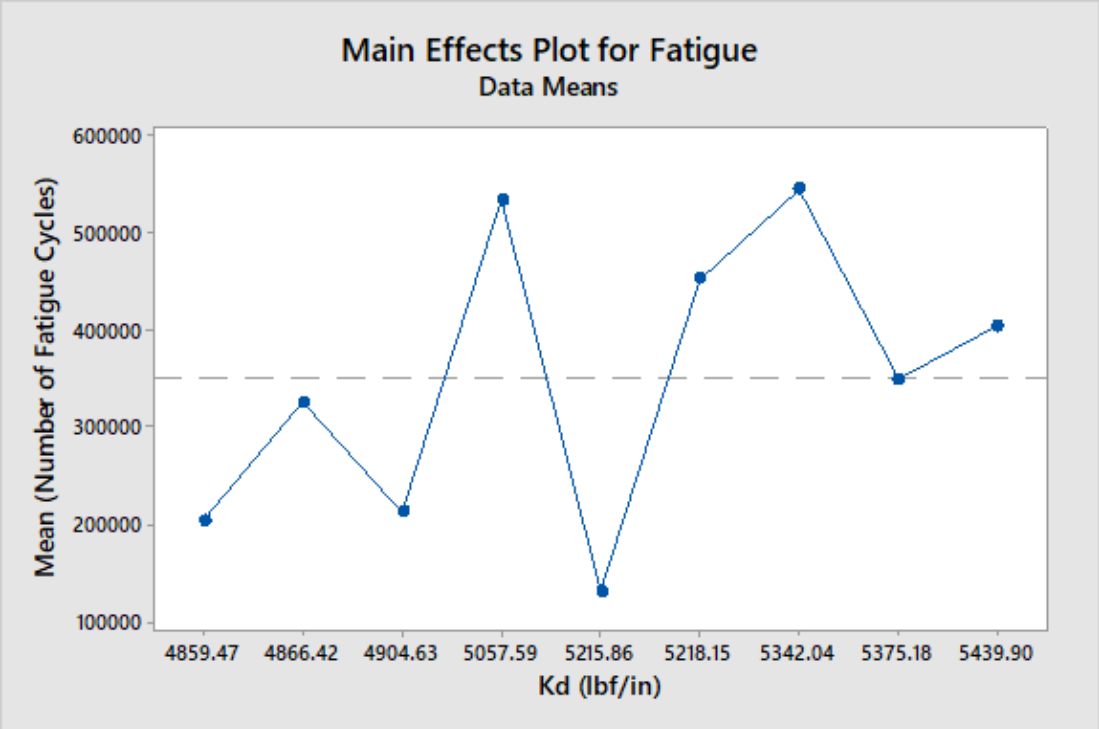

Figure 4.11: Fatigue Versus Dynamic Stiffness

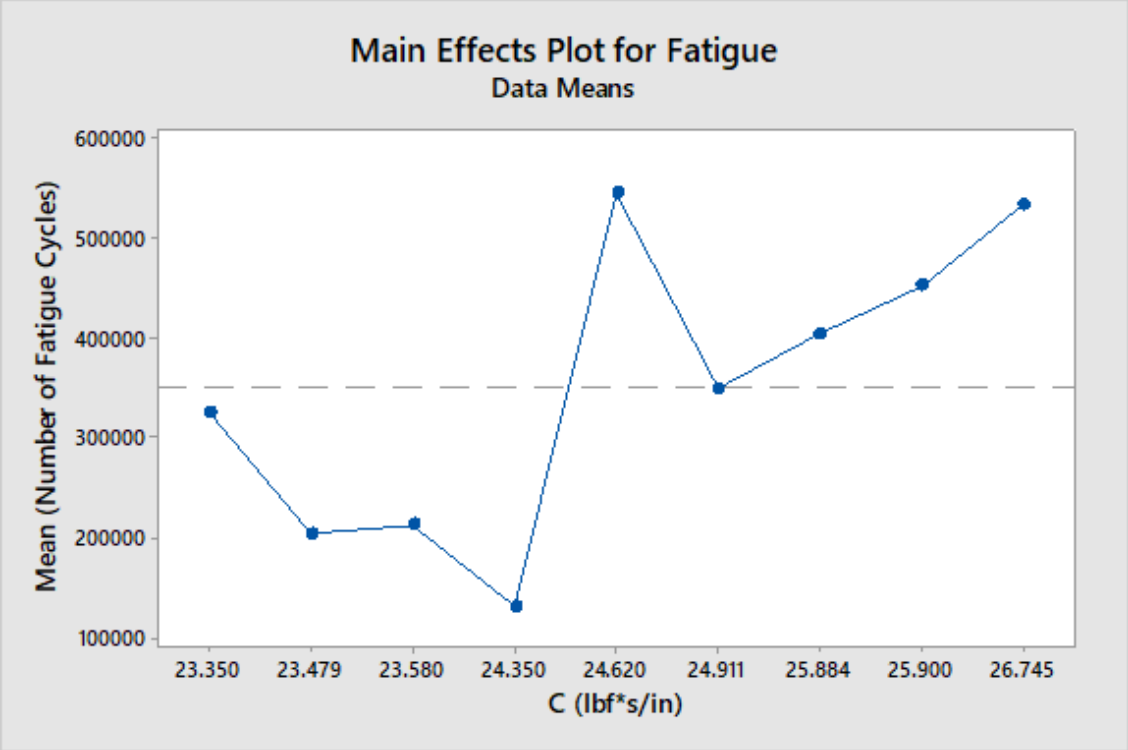

Figure 4.12: Fatigue Versus Damping

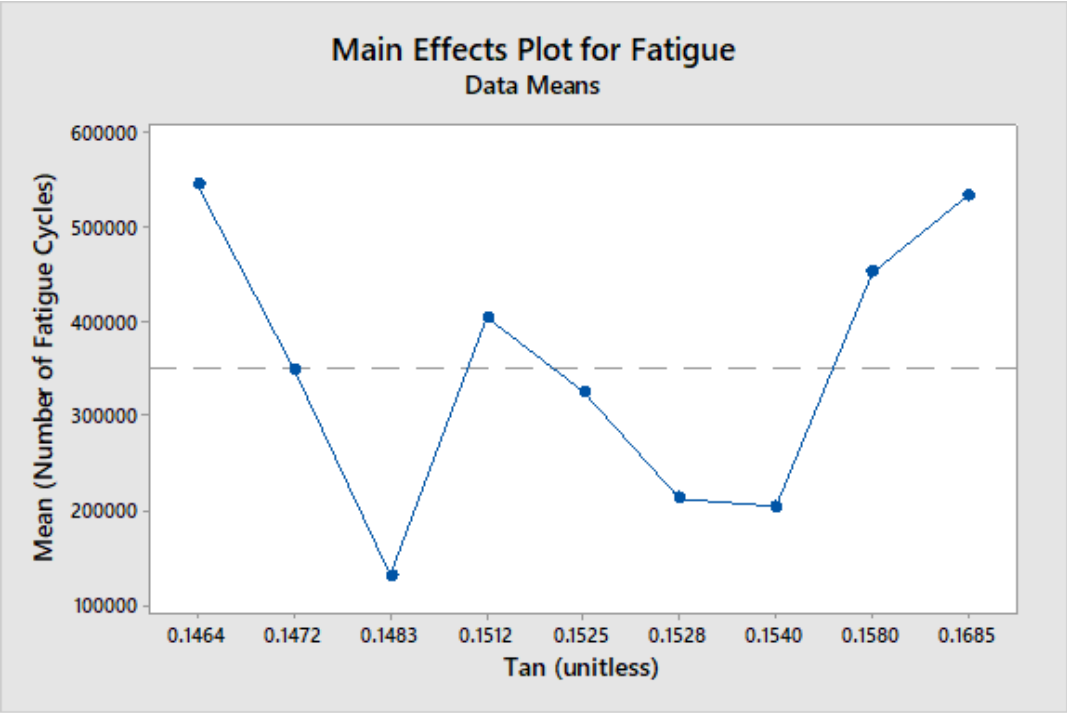

Figure 4.13: Fatigue Versus Tan Delta

The new design of experiment has greater consistency in the fatigue results in that there are fewer outliers than the original experiment. It is believed that this consistency was due to the improved sample specimen. The failure mode seen during the new experiment was caused by rubber fatigue failure, and not a failure due to the rubber slicing over the steel plates. The new experiment also used the help of finite element analysis to determine whether the part would compress symmetrically and only produce one crease. The crease information from the finite element analysis helped ensure that the fatigue failure mode would occur in the middle section of the part, thus making the fatigue test repeatable.

The results obtained from the new experiment do show more correlation between the nondestructive test results and the destructive test result when comparing them to the original experiment. Furthermore, there were fewer outliers since none of the new sample specimens needed to be hit out of the mold with a hammer. Therefore, the results were more repeatable then the original experiment. It is advised that future work should continue to test sample specimens in this nature.

CHAPTER 5

CONCLUSION AND FUTURE WORK

The inconsistencies found in the data (fatigue variability) can be attributed to the rubber being folded over the steel plates in the sample, and not from pure rubber failure. Therefore, even though the experimental procedure was well designed, the sample specimen design was flawed. The reason behind choosing this specimen was because parts with a similar shape are used in heavy-duty suspension systems. The design of the experiment is not completely lost though. Sufficient data can be seen that shows a drop off in fatigue when the cure time exceeds nominal state of cure. Furthermore, if a rubber part must be forced (hit) out of the mold when the manufacturing process is complete, that part should be scrapped. Also, lot to lot variation is very minimal because the time between the shipments of rubber lots is only two weeks. Perhaps a seasonal spread between lots may produce different results.

Additional data shows that static stiffness and damping are optimized at the nominal state of cure and that tan delta increases as cure time increases. This data is consistent with the literature. Because the fatigue data was inconsistent, correlations between the nondestructive test results and the destructive test results cannot be made. However, the techniques used in this thesis can be applied to future tests that. The graphical approach is perhaps the easiest and most efficient technique to visually interpret data that is taken from samples. Similarly, the regression models created from Minitab can accurately predict some measures such as static stiffness and damping given the cure time and temperature used to make the part.

The graphical approach is recommended to be used to visually infer the correlations between fatigue and the different combinations of cure time and temperature. Similarly, regression equations will be created to predict nondestructive and destructive test results based on the data produced from the new samples.

Other experiments that can be done using this experimental design include:

- Holding the cure parameters constant and change the loading of the fatigue test (i.e., using 20,000lb instead of 15,000lb). This experiment would show how fast the component fails if it is overloaded. The data provided from this experiment would help show customers the decreased longevity of the overall suspension system if it is overloaded with material.
- Changing the failure criteria to a larger percentage of loss in static stiffness. This experiment would be like the previous experiment stated but it would should how the rubber responds when it is loaded for a longer period of time. Will there be a sharp decrease in compressive stiffness once a 40% loss in stiffness is reaches? Questions like these can be answered with this experiment.
- Testing different durometers of rubber. This thesis used a 70-durometer rubber; however, different nondestructive and destructive test data will help determine the best rubber material to be used in suspension system components.

- Producing different shaped sample specimens to determine the optimal shape for a rubber component. Because of the inconsistencies of the fatigue data, the inconsistencies may not concern the cure parameters, but may be associated with the actual design of the rubber component. This type of experiment may be costly to run based on the number of molds that has to be produced, but invaluable insight may be achieved. The new design of experiment was a great first step.

Overall, even though the experiment conducted in this thesis could not answer all the questions that it should have been able to, many takeaways were produced. The design of experiment created, and the analysis methods used, can be utilized in the future work of this thesis. However, with all the factors that are associated with rubber processing, the design of experiment created in this thesis may not be the ultimate answer to maximizing fatigue life. Mainly, shape may be a bigger factor than any of the processing parameters, but again, that is a very expensive endeavor.

The new design of experiment did show some promise in obtaining more consistent fatigue life results. Future work should start by testing more samples using the new design of experiment and the new sample specimen to obtain fatigue results that are statistically significant (i.e. a sample size of six for each cure parameter combination).

BIBLIOGRAPHY

[1] G.J. Lake and P.B. Lindley. "Mechanical fatigue limit for rubber." *Journal of Applied Polymer Science.* Vol. 9, pg. 1233, 1965.

[2] A. Ansarifar, N. Ibrahim. And M. Bennett. "Reinforcement of natural rubber with silanized precipitated silica nanofiller." *Rubber Chemistry and Technology.* Vol. 78, No. 5, 2005.

[3] John G. Sommer Jr, inventor; The General tire & Rubber Company, assignee. *Method of improving fatigue life of molded sulfur-cured rubber articles.* US patent 3,913,209, 1975.

[4] B. T. Poh, M. F. Chen, and B. S. Ding. "Cure Characteristics of Unaccelerated Sulfur Vulcanization of Epoxidized Natural Rubber." *Journal of Applied Polymer Science,* Vol. 60, pp. 1569-1574. 1996.

[5] P. Posada, A. Fernandez-Torres, J. L. Valentin, A. Rodriguez, L. Gonzalez. "Effect of the Temperature on the Kinetic of Natural Rubber Vulcanization with the Sulfur Donor Agent Dipentamethylene Thiuram Tetrasulphide." *Journal of Applied Science.* Vol. 115, pp. 692-701. 2010.

[6] W.V. Mars. "Fatigue life predictions for elastomeric structures." *Presented at the Spring Division, ACS, Meeting.* Akron, Ohio, April 30- May 2, 2007.

[7] W.V. Mars and A. Fatemi. Multiaxial fatigue of rubber: "Part 1: equivalence criteria and theoretical aspects." *Research and Technology Department, Cooper Tire and Rubber Company.* Findlay, Ohio. 20 January 2005.

[8] W.V. Mars and A. Fatemi. "A literature survey on fatigue analysis approaches for rubber." *International Journal of Fatigue*, Vol. 24, pp. 949-961, 2002.

[9] G. Ayoub, M. Nait-Abdelaziz, F. Zairi, J.M. Gloaguen, and P. Charrier. "A continuum damage model for high-cycle fatigue life prediction of styrene-butadiene rubber under multiaxial loading." *International Journal of Solids and Structures*. Vol. 48, pp. 2458-2466, 2011.

[10] A. N. Gent, P. B. Lindley, and A. G. Thomas. "Cut growth and fatigue of rubbers. I. The relationship between cut growth and fatigue." *Journal of Applied Polymer Science.* No. 8, pg. 455, 1964.

[11] Xiao-Li Wang, Wen-Bin Shangguan, Subhash Rakheja, Wu-Cjeng Li, and Bin Yu. "A method to develop a unified fatigue life prediction model for filler natural rubbers under uniaxial loads." *Fatigue and Fracture of Engineering Materials and Structures.* 26 July 2013.

[12] W.V. Mars and A. Fatemi. “Factors that affect Fatigue Life of Rubber: a Literature Survey.” *Journal of Rubber Chemistry and Technology.* Vol. 77, No. 3, pp 391-412, 2004.

[13] W. V. Mars and A. Fatemi. “Observations of the constitutive response and characterization of filled natural rubber under monotonic and cyclic multiaxial stress states.” *Journal of Engineering Materials and Technology.* Vol. 126, pp. 19-28, January 2004.

[14] W. V. Mars and A. Fatemi. “Multiaxial fatigue of rubber: Part II: experimental observations and life predictions.” *Fatigue and Fracture of Engineering Materials and Structures.* Vol. 28, pp. 523-538, April 2005

[15] R.J. Harbour, A. Fatemi, and W.V. Mars. “Fatigue life analysis and predictions for NR and SBR under variable amplitude and multiaxial loading conditions.” *International Journal of Fatigue.* 30, pp 1231-1247, 2008

[16] K. N. G. Fuller, J. Gough, and A. G. Thomas. “The effect of low-temperature crystallization on the mechanical behavior of rubber.” *Journal of Polymer Science: Part B: Polymer Physics.* Vol. 42, pp. 2181-2190, 2004.

[17] W. V. Mars. “Analysis of stiffness variations in context of strain-stress, and energy controlled processes.” *Rubber Chemistry and Technology*, Vol. 84, No.2, pp. 178 186. 2011.

[18] S. M. Cadwell, R. A. Merrill, C. M. Sloman, and F.L. Yost. “Dynamic fatigue life of rubber.” *Industrial and Engineering Chemistry, Analytical Edition*, Vol. 12, No. 1, pp 19-23, January 1940.

[19] C. M. Roland. “Mechanical behavior of rubber at high strain rates.” *Chemistry Division, Naval Research Laboratory.* Vol. 79, No.3, pp. 429-459, July 2006

[20] A.N. Gent and M. Hindi. “Heat Build-up and Blowout of Rubber Blocks.” *Presented at a meeting of the Rubber, Division, American Chemical Society.* Dallas, Texas, 19 22, 1988.

[21] W.V. Mars and A. Fatemi. “Analysis of fatigue life under complex loading revisiting Cadwell, Merill, Sloman, and Yost.” *Presented at a meeting of the Rubber Division, American Chemical Society.* Grand Rapids, Michigan, May 17-19, 2004

[22] C. Sun, A. Gent, and P. Marteny. “Effect of Fatigue Step Loading Sequence on Residual Strength.” *Presented at the eighteenth annual conference of The Tire Society.* Akron, Ohio, April 27-28, 1999

[23] T. Steinweger, M. Flamm, and U. Weltin. “A methodology for test time reduction in rubber part testing.” *Constitutive Models for Rubber III*, 2003.

[24] W.V. Mars and A. Fatemi. “A phenomenological model for the effect of R ratio on fatigue of strain crystallizing rubbers.” *Presented at the Rubber Division, ACS, Fall Meeting*. October 8-11, 2002.

[25] R. J. Harbour, A. Fatemi, and W. V. Mars. “The effect of a dwell period on fatigue crack growth rates in filled SBR and NR.” *Presented at the Fall Rubber Division, ACS, Meeting.* October 10-12, 2006.

[26] P. B. Lindley. “Relation between hysteresis and the dynamic crack growth resistance of natural rubber.” *International Journal of Fracture*, Vol. 9, No. 4, December 1973.

[27] K Tsunoda. “Fatigue testing methods for elastomers.” *Nippon Gomu Kyokaishi.* No. 1, pp. 20-27, 2010.

[28] Compression Set, Creep and Stress Relaxation. *Gallagher Corporation.* 24 Jan. 2017. Web. 12 Jan. 2018.

[29] Creep and Stress Rupture Properties. *NDT Resource Center.* Web. 12 Jan. 2018.

APPENDIX A

Nondestructive Testing Procedures

Four nondestructive tests used to determine the performance of the rubber in suspension systems. These tests were run on the MTS-810 machine by the test engineer at Hendrickson's manufacturing plant in Kendallville, Indiana. This appendix outlines how these tests are defined and performed. Also note that the data analysis of the four nondestructive tests can be seen below.

A.1 Static Stiffness, K_s

Static stiffness is measured by tracking the pound force applied to the specimen as well as the displacement corresponding to the load. The average load per displacement is calculated to find the final static stiffness rating.

A.2 Dynamic Stiffness, K_d

Dynamic stiffness is measured by taking the average dynamic load peak to peak, and dividing that by the average peak to peak displacement.

A.3 Damping, C

Damping is calculated by taking the static stiffness rate, multiplying it by the sine of the phase angle, which is the phase shift between in the input force wave and the

output displacement wave, and dividing it by two-pi and the frequency at which the test is run.

A.4 Tan Delta

Tan delta is found by taking the tangent of the phase angle between the input force wave and the output displacement wave. All the data is tracked and sent to an Excel sheet where all the calculations can be made.

A.5 Nondestructive Tests

To determine the parameters' effect on the nondestructive tests, a similar approach was also taken with the nondestructive tests. While the goal of this study was to look at fatigue, the availability of the nondestructive test data provided an opportunity to understand how the processing parameters could also be used in other analyses. Thus, the test results are provided to complete the analysis.

There were 4 nondestructive measures used: static stiffness (K_s), dynamic stiffness (K_d), damping (C), and tan delta. Static stiffness is a major consideration by Hendrickson because their suspensions carry very heavy loads and each of their rubber components must be able to carry loads without rupturing. Even though damping is not a major parameter, the test data confirms that damping has similar optimization parameters to static stiffness. It also helps confirm that the test setup produces consistent results. Although damping does not affect the load carrying capacity of the suspension system, it does affect the ride quality. The rubber components in suspensions are often used to help create a smooth drive for the truck driver.

The analysis of the nondestructive tests can be seen in Appendix A. The correlation between the nondestructive test results and the destructive test results can be seen below.

A.5.1 Graphical Approach

To analyze the results from the non-destructive tests, a graphical approach was also performed. In order to determine optimal combinations of state of cure and cure temperature that produce optimal nondestructive test parameters, interaction plots were produced comparing each combination of state of cure and cure temperature with each of the nondestructive test parameters. Figures B.3-B.10 (Appendix B) show these interactions. These plots provide a framework to produce similar parts with similar nondestructive test results. Hendrickson will be able to use these plots to pinpoint exactly what cure temperature and state of cure to use to produce parts with these nondestructive test parameter values.

A.5.1.1 Static Stiffness

Figure B.3 (Appendix B) shows the interaction plot for static stiffness. Static stiffness is optimized at states of cure 2 (slightly under) and 3 (nominal), then drops off as the state of cure increases. Also note that static stiffness is not influenced by cure temperature, so the only main effect is state of cure. The interval plot (Figure B.4 (Appendix B)) shows that there is a large spread in the data is relatively small (<10%).

A.5.1.2 Dynamic Stiffness

As seen in Figures B.5 and B.6 (Appendix B), dynamic stiffness is optimized when the state of cure is 3 (nominal cure), regardless of cure temperature. Therefore, dynamic stiffness is only influenced by the state of cure, resulting in a main effect.

A.5.1.3 Damping

Because damping is a function of dynamic stiffness and the frequency at which the component is tested, Figures B.7 and B.8 (Appendix B) look very similar to Figures B.3 and B.4 (Appendix B). Damping is maximal at state of cure 3 (nominal cure), and the cure temperature does not affect the results.

A.5.1.4 Tan Delta

Different than static stiffness and damping, tan delta is maximal at state of cure 5 (over cure). As seen in Figures B.9 and B.10 (Appendix B), there is a linear correlation between tan delta and state of cure, and the cure temperature does not have a significant effect on tan delta.

A.5.2 Regression approach

A.5.2.1 Static Stiffness

In addition to predicting fatigue, the nondestructive test parameters can also be predicted using the same process for predicting fatigue. Below, Equation 2 is used to predict the static stiffness measured in $\frac{lbf}{in}$:

$$Ks = 22532 + 371\,Cure\,Temp_{170} - 371\,Cure\,Temp_{175} + 434\,State\,of\,Cure_1 + 1101\,State\,of\,Cure_2 + 1596\,State\,of\,Cure_3 - 812\,State\,of\,Cure_4 - 2320\,State\,of\,Cure_5 + 148\,Cure\,Temp_{170} * State\,of\,Cure_1 - 435\,Cure\,Temp_{170} * State\,of\,Cure_2 - 59\,Cure\,Temp_{170} * State\,of\,Cure_3 - 51\,Cure\,Temp_{170} * State\,of\,Cure_4 + 397\,Cure\,Temp_{170} * State\,of\,Cure_5 - 148\,Cure\,Temp_{175} * State\,of\,Cure_1 + 435\,Cure\,Temp_{175} * State\,of\,Cure_2 + 59\,Cure\,Temp_{175} * State\,of\,Cure_3 + 51\,Cure\,Temp_{175} * State\,of\,Cure_4 - 397\,Cure\,Temp_{175} * State\,of\,Cure_5$$

Similar analysis can be done with this equation for static stiffness as was done with fatigue. The parameter that has the largest effect on static stiffness is state of cure 5 (over cure) (-2320). In addition, to achieve maximum static stiffness, having a cure temperature of 170 degrees Celsius with a state of cure 3 (nominal cure) will create a sample with static stiffness of approximately 24,440 $\frac{lbf}{in}$. The regression equation is consistent with the graphical approach where static stiffness is the highest at a cure temperature of 170 degrees Celsius and a state of cure of 3 (nominal cure).

A.5.2.2 Dynamic Stiffness

Equation 3 below is generated to predict dynamic stiffness in units of $\frac{lbf}{in}$.

$$Kd5 = 33898 + 615\,Cure\,Temp_{170} - 615\,Cure\,Temp_{175} - 11\,State\,of\,Cure_1 + 1327\,State\,of\,Cure_2 + 2250\,State\,of\,Cure_3 - 851\,State\,of\,Cure_4 - 2715\,State\,of\,Cure_5 + 401\,Cure\,Temp_{170} * State\,of\,Cure_1 - 562\,Cure\,Temp_{170} * State\,of\,Cure_2 - 66\,Cure\,Temp_{170} * State\,of\,Cure_3 - 130\,Cure\,Temp_{170} * State\,of\,Cure_4 + 357\,Cure\,Temp_{170} * State\,of\,Cure_5 - 401\,Cure\,Temp_{175} * State\,of\,Cure_1 + 562\,Cure\,Temp_{175} * State\,of\,Cure_2 + 66\,Cure\,Temp_{175} * State\,of\,Cure_3 + 130\,Cure\,Temp_{175} * State\,of\,Cure_4 - 357\,Cure\,Temp_{175} * State\,of\,Cure_5 \quad (3)$$

The cure parameter that influences dynamic stiffness the most is state of cure 5 (over cure) (-2715). The largest dynamic stiffness is found when the cure temperature is 170 degrees Celsius and a state of cure of 3 (nominal cure) (36,697 $\frac{lbf}{in}$). Also note that

this combination of cure temperature and state of cure produces the largest dynamic stiffness using the graphical approach as well.

A.5.2.3 Damping

Equation 4 below is generated to predict damping in units of $\frac{lbf*s}{in}$:

$$\begin{aligned} C5 = {} & 176.462 + 3.763\ Cure\ Temp_{170} - 3.7\ Cure\ Temp_{175} - 6.71\ State\ of\ Cure_1 \\ & + 1.61\ State\ of\ Cure_2 + 9.97\ State\ of\ Cure_3 - 0.57\ State\ of\ Cure_4 \\ & - 4.30\ State\ of\ Cure_5 + 4.92\ Cure\ Temp_{170} * State\ of\ Cure_1 \\ & - 1.73\ Cure\ Temp_{170} * State\ of\ Cure_2 - 0.87\ Cure\ Temp_{170} * State\ of\ Cure_3 \\ & - 0.99\ Cure\ Temp_{170} * State\ of\ Cure_4 - 1.33\ Cure\ Temp_{170} * State\ of\ Cure_5 \\ & - 4.92\ Cure\ Temp_{175} * State\ of\ Cure_1 + 1.73\ Cure\ Temp_{175} * State\ of\ Cure_2 \\ & + 0.87\ Cure\ Temp_{175} * State\ of\ Cure_3 + 0.99\ Cure\ Temp_{175} * State\ of\ Cure_4 \\ & + 1.33\ Cure\ Temp_{175} * State\ of\ Cure_5 \end{aligned} \quad (4)$$

The cure parameter that affects damping the most is state of cure 3 (nominal cure), which has a coefficient of 9.97. Furthermore, the combination that produces maximum damping is a cure temperature of 170 and a state of cure 3 (nominal cure), which has a value of 189.325 $\frac{lbf*s}{in}$.

A.5.2.4 Tan Delta

Finally, Equation 5 is generated to predict tan delta, where the units are unitless:

$$\begin{aligned} Tan5 = {} & 0.166067 + 0.000441\ Cure\ Temp_{170} - 0.000441\ Cure\ Temp_{175} \\ & - 0.006854\ State\ of\ Cure_1 - 0.005138\ State\ of\ Cure_2 \\ & - 0.001820\ State\ of\ Cure\_3 + 0.003608\ State\ of\ Cure\_4 \\ & + 0.010203\ State\ of\ Cure_5 + 0.002950\ Cure\ Temp_{170} * State\ of\ Cure_1 \\ & + 0.001215\ Cure\ Temp_{170} * State\ of\ Cure_2 \\ & - 0.000385\ Cure\ Temp_{170} * State\ of\ Cure_3 \\ & - 0.000233\ Cure\ Temp_{170} * State\ of\ Cure_4 \\ & - 0.003547\ Cure\ Temp_{170} * State\ of\ Cure_5 \\ & - 0.002950\ Cure\ Temp_{175} * State\ of\ Cure_1 \\ & - 0.001215\ Cure\ Temp_{175} * State\ of\ Cure_2 \\ & + 0.000385\ Cure\ Temp_{175} * State\ of\ Cure_3 \\ & + 0.000233\ Cure\ Temp_{175} * State\ of\ Cure_4 \end{aligned} \quad (4)$$

$$+ 0.003547\ Cure\ Temp_{175} * State\ of\ Cure_5$$

To achieve the highest tan delta value, the combination of cure temperature and state of cure that must be used is 170 degrees Celsius and 5, respectively. This combination produces a tan delta value of approximately 0.179817. Also note, having a state of cure of 5 (over cured) affects tan delta the greatest (0.010203).

A.5.3 Tabular Approach

ANOVA tables were created similar to the one for the regression equation for fatigue for the nondestructive test parameters. The p-values generated for the corresponding experiments are much lower than the ones for fatigue. These low p-values show that the cure parameters significantly affect the nondestructive test parameters. In addition, the residuals for each of the nondestructive test parameters are very small compared to fatigue. The low residual values show that the regression equations created can predict the values accurately.

A.5.3.1 Static Stiffness

Table B.3 (Appendix B) shows the ANOVA table for static stiffness. Parameters that have a significant effect on fatigue are states of cure 2 (slightly under), 3 (nominal cure), and 5 (over cure).

A.5.3.2 Dynamic Stiffness

As seen in Table B.4 (Appendix B), the p-values for states of cure 1 (under), 3 (nominal), and 5 (over) are lower than 0.05, which shows that states of cure 1 (under), 3 (nominal), and 5 (over) have a significant effect on dynamic stiffness. Figure B.11

(Appendix B) reveals that the residuals for dynamic stiffness are much smaller than those for fatigue.

A.5.3.3 Damping

Similar to dynamic stiffness, states of cure 1 (under) and 3 (nominal) have a p-value less than 0.05 (Table B.5 (Appendix B)). In addition, the residuals are very small, which shows that the fitted equation closely predicts the actual values of damping (Figure B.12 (Appendix B)).

A.5.3.4 Tan Delta

Equation #5, which is generated above, is a great fit to the actual data because the p-value for most of the coefficients are less than 0.05, as seen in Table B.6 (Appendix B). In addition, the residual plots show that the residuals are very small, and are normally distributed in the histogram, which reinforces that the equation is a good fit (Figure B.13 (Appendix B)).

APPENDIX B

Experimental Results

This appendix documents the experimental results of the tests.

Table B.1: Summary of Results Example

Sample ID	Cure Temp (°C)	Cure Time (min)	Static Rate (lbf/in)	K* @ 5Hz (lbf/in)	C @ 5Hz (lbf-sec/in)	Tan Δ @ 5Hz (unitless)	Durability Life (cycles)
001	170	2.5	23731	35631	185	0.1657	270,600
002	170	2.5	23491	34848	179	0.1631	232,000
003	170	2.5	23234	34230	171	0.1593	230,900
005	170	2.5	22703	33329	164	0.1569	186,500

Figure B.1: MTS Test Setup

Table B.2: ANOVA Table for Fatigue

Term	Coef	SE Coef	T-Value	P-Value
Constant	195223	8617	22.66	0.000
	Cure Temp			
170	3890	8617	0.45	0.655
175	-3890	8617	-0.45	0.655
	State of Cure			
1	26002	16238	1.60	0.119
2	31894	17365	1.84	0.075
3	-6198	17365	-0.36	0.723
4	-18665	17365	-1.07	0.290
5	-33033	17796	-1.86	0.072
	Cure Temp*State of Cure			
170 1	-16565	16238	-1.02	0.315
170 2	-21440	17365	-1.23	0.225
170 3	19535	17365	1.12	0.268
170 4	-7949	17365	-0.46	0.650
170 5	26420	17796	1.48	0.147
175 1	16565	16238	1.02	0.315
175 2	21440	17365	1.23	0.225
175 3	-19535	17365	-1.12	0.268
175 4	7949	17365	0.46	0.650
175 5	-26420	17796	-1.48	0.147

.

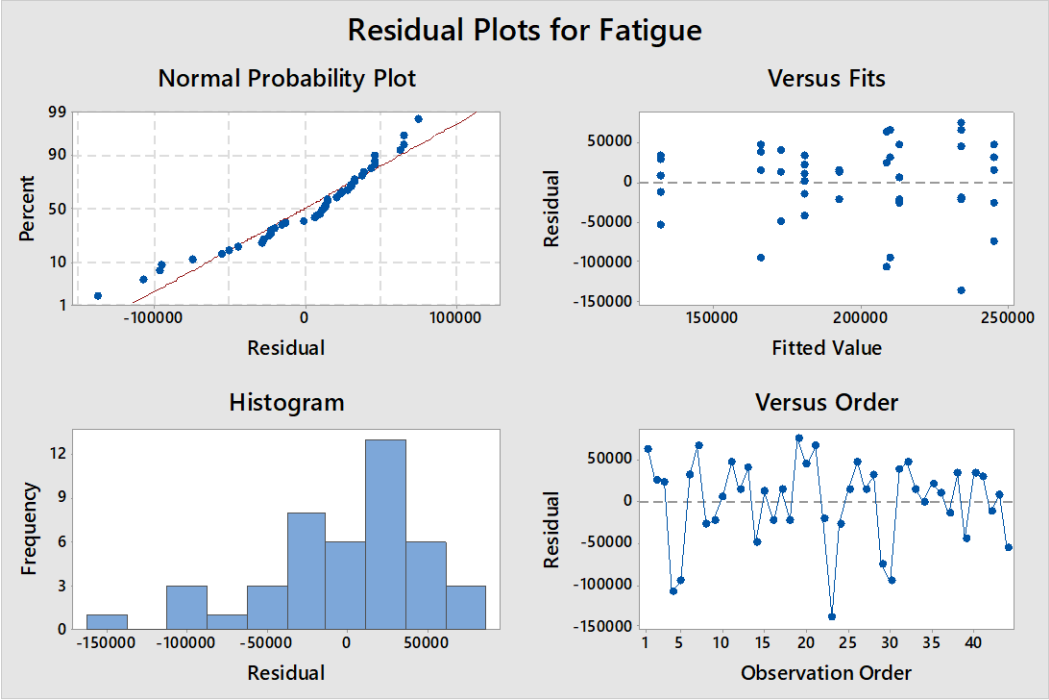

Figure B.2: Residual Plots for Fatigue with State of Cure and Cure Temperature as Factors

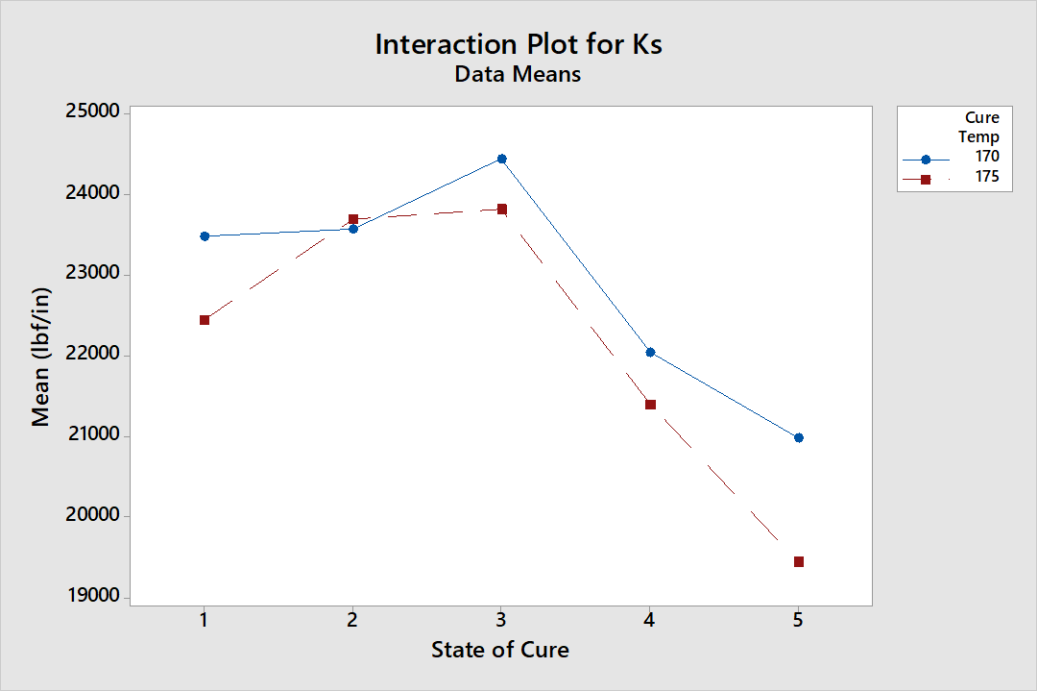

Figure B.3: Interaction Plot of State of Cure and Cure Temperature for Static Stiffness

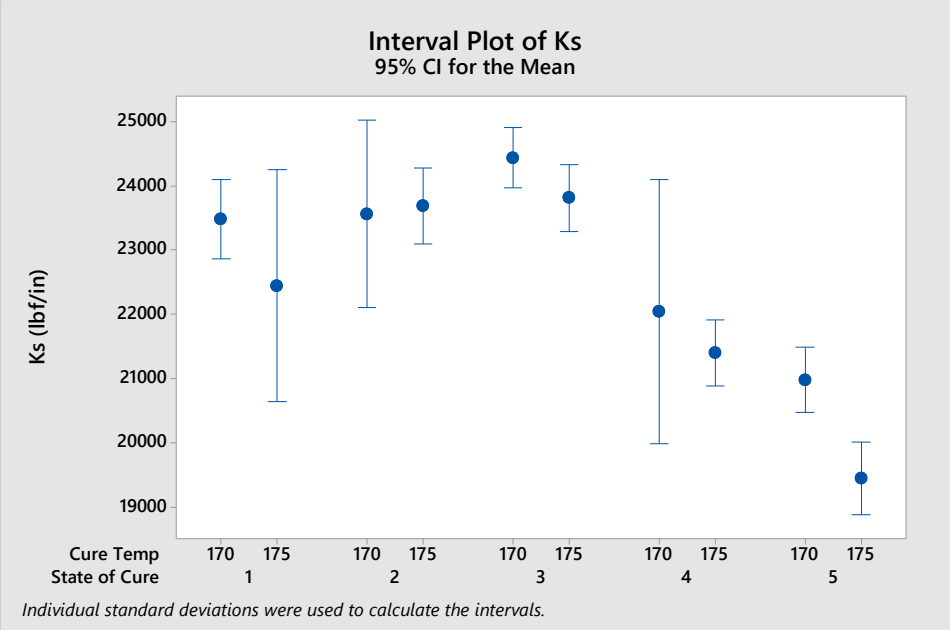

Figure B.4: Variation Plot of State of Cure and Cure Temperature for Static Stiffness

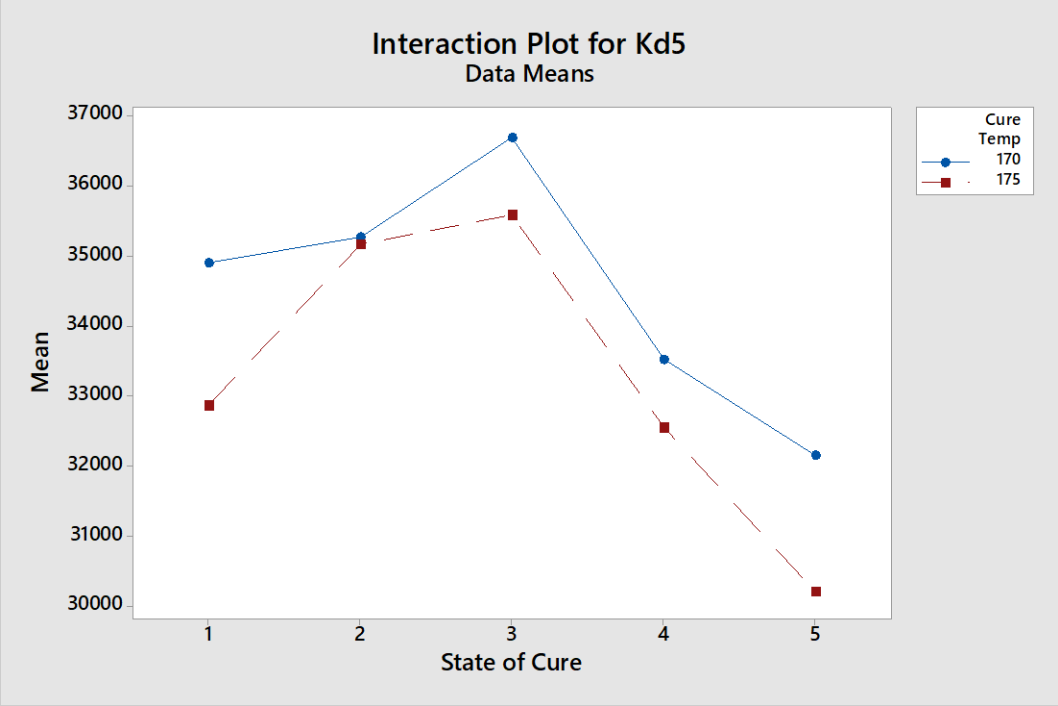

Figure B.5: Interaction Plot of State of Cure and Cure Temperature for Dynamic Stiffness at 5Hz

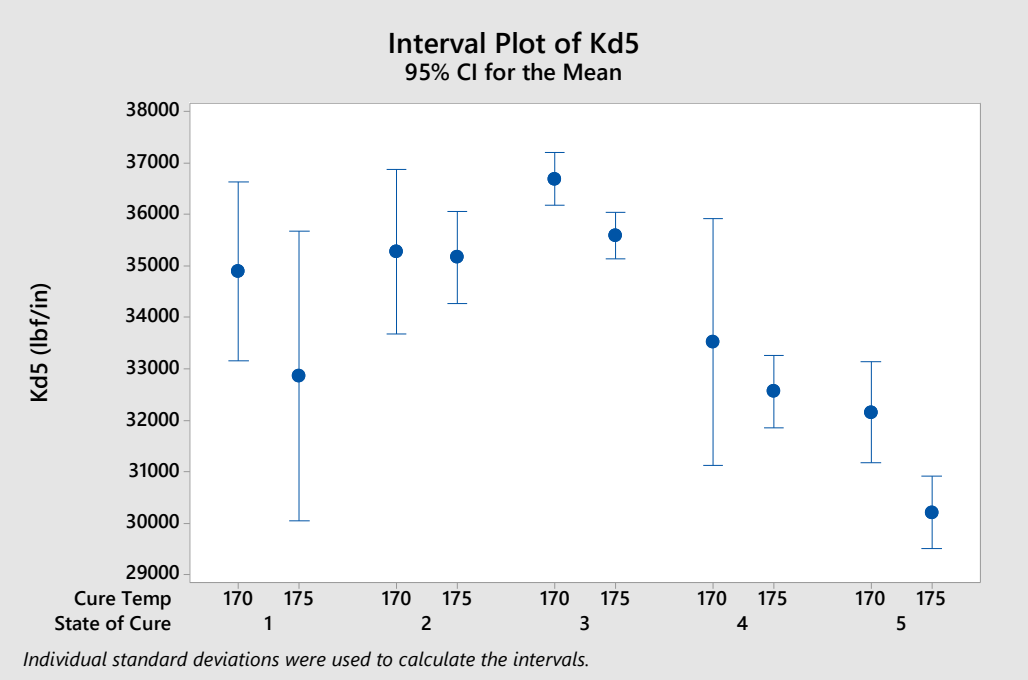

Figure B.6: Variation Plot of State of Cure and Cure Temperature for Dynamic Stiffness at 5Hz

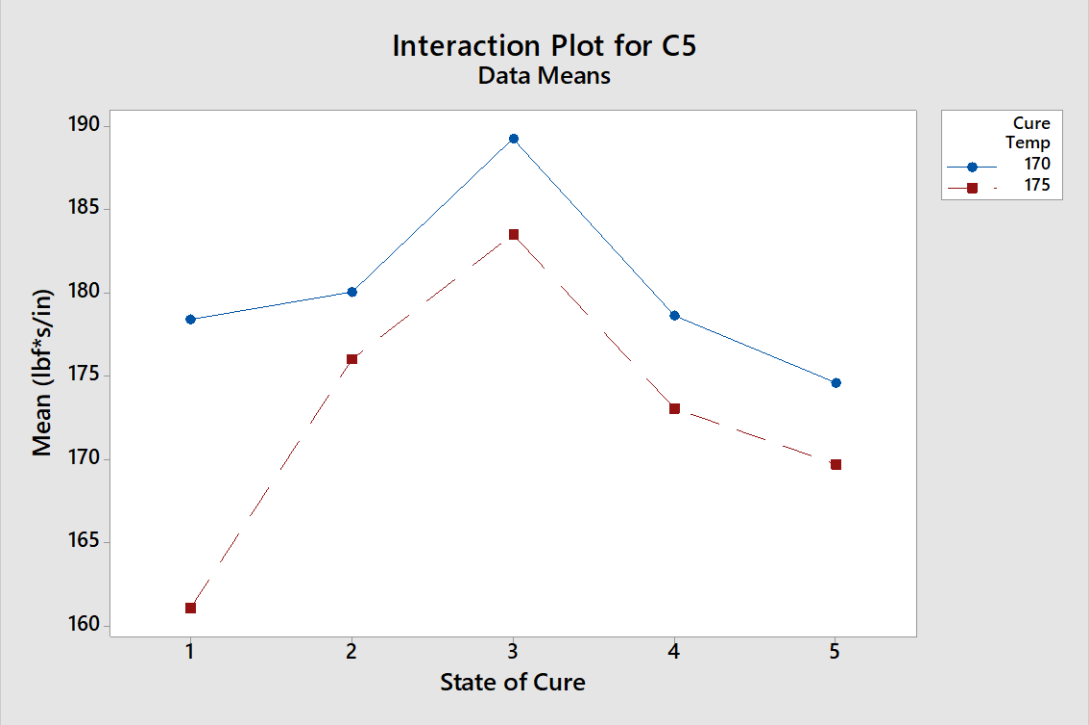

Figure B.7: Interaction Plot of State of Cure and Cure Temperature for Damping at 5Hz

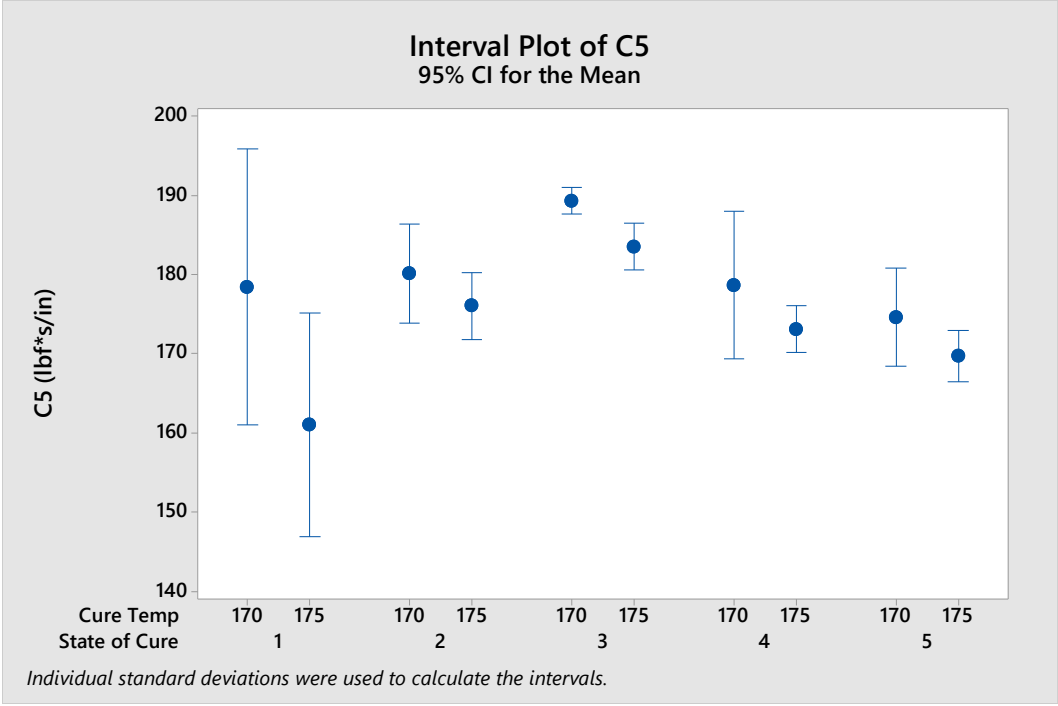

Figure B.8: Variation Plot of State of Cure and Cure Temperature for Damping at 5Hz

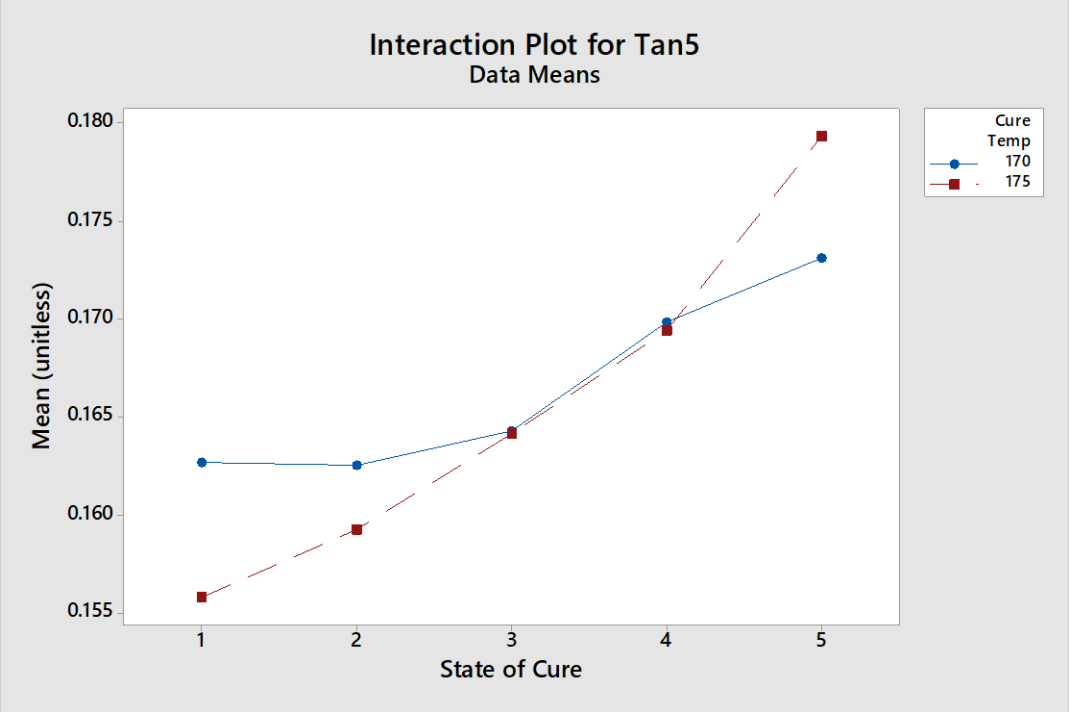

Figure B.9: Interaction Plot of State of Cure and Cure Temperature for Tan Delta at 5Hz

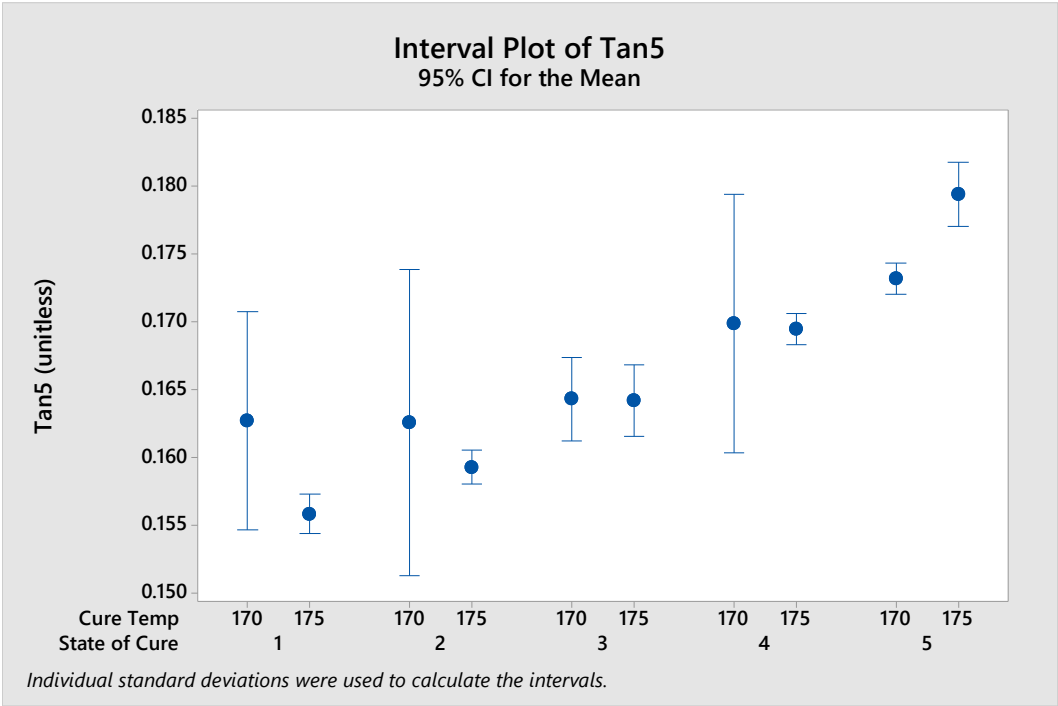

Figure B.10: Variation Plot of State of Cure and Cure Temperature for Tan Delta at 5Hz

Table B.3: ANOVA Table for Static Stiffness

Term	Coef	SE Coef	T-Value	P-Value
Constant	22226	310	71.69	0.000
Cure Temp				
170	66	310	0.21	0.833
175	-66	310	-0.21	0.833
State of Cure				
1	-788	584	-1.35	0.186
2	1407	625	2.25	0.031
3	1901	625	3.04	0.004
4	-506	625	-0.81	0.424
5	-2014	640	-3.15	0.003
Cure Temp*State of Cure				
170 1	-1075	584	-1.84	0.075
170 2	-130	625	-0.21	0.837
170 3	247	625	0.40	0.695
170 4	255	625	0.41	0.686
170 5	703	640	1.10	0.280
175 1	1075	584	1.84	0.075
175 2	130	625	0.21	0.837
175 3	-247	625	-0.40	0.695
175 4	-255	625	-0.41	0.686
175 5	-703	640	-1.10	0.280

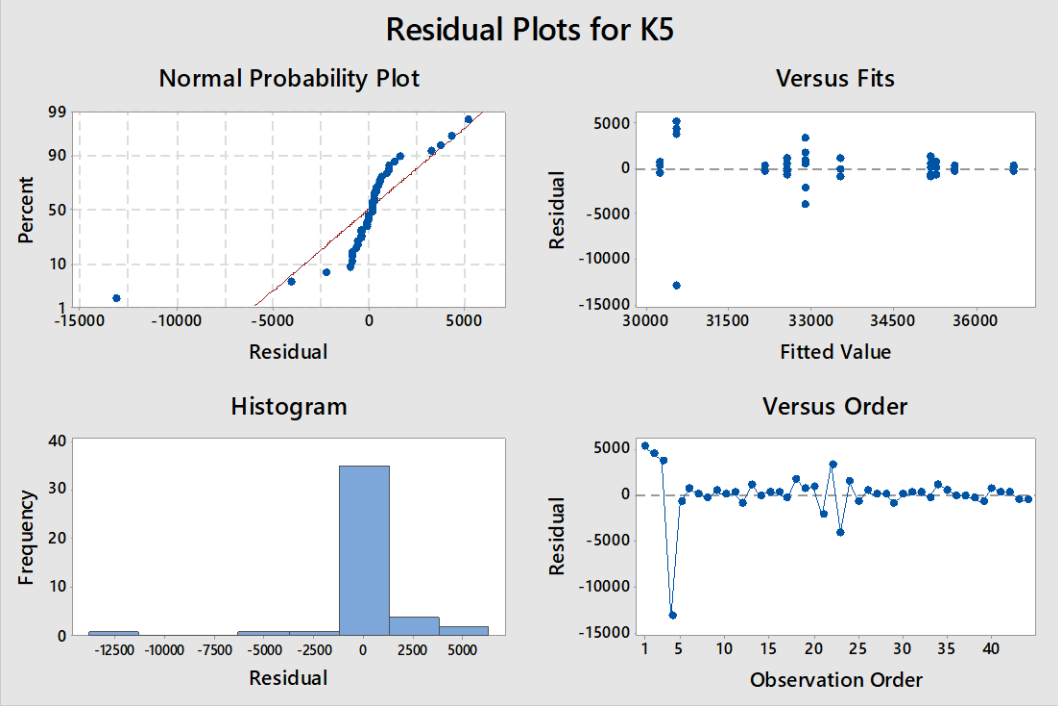

Figure B.11: Residual Plots for Dynamic Stiffness with State of Cure and Cure Temperature as Factors

Table B.4: ANOVA Table for Dynamic Stiffness

Term	Coef	SE Coef	T-Value	P-Value
Constant	33459	449	74.60	0.000
Cure Temp				
170	176	449	0.39	0.697
175	-176	449	-0.39	0.697
State of Cure				
1	-1767	845	-2.09	0.044
2	1766	904	1.95	0.059
3	2689	904	2.98	0.005
4	-412	904	-0.46	0.651
5	-2276	926	-2.46	0.019
Cure Temp*State of Cure				
170 1	-1355	845	-1.60	0.118
170 2	-123	904	-0.14	0.893
170 3	373	904	0.41	0.682
170 4	309	904	0.34	0.735
170 5	796	926	0.86	0.396
175 1	1355	845	1.60	0.118
175 2	123	904	0.14	0.893
175 3	-373	904	-0.41	0.682
175 4	-309	904	-0.34	0.735
175 5	-796	926	-0.86	0.396

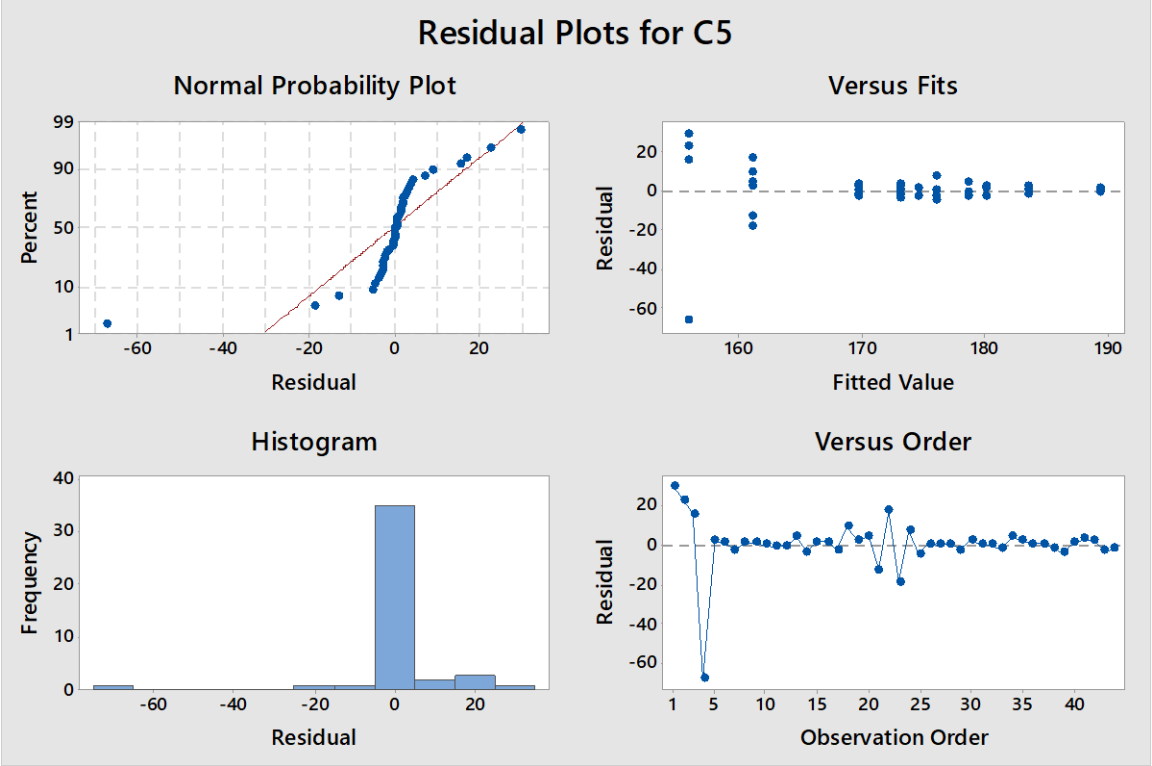

Figure B.12: Residual Plots for Damping with State of Cure and Cure Temperature as Factors

Table B.4: ANOVA Table for Damping

Term	Coef	SE Coef	T-Value	P-Value
Constant	174.21	2.29	75.96	0.000
Cure Temp				
170	1.51	2.29	0.66	0.514
175	-1.51	2.29	-0.66	0.514
State of Cure				
1	-15.72	4.32	-3.64	0.001
2	3.86	4.62	0.84	0.409
3	12.22	4.62	2.64	0.012
4	1.68	4.62	0.36	0.719
5	-2.05	4.74	-0.43	0.668
Cure Temp*State of Cure				
170 1	-4.08	4.32	-0.95	0.351
170 2	0.52	4.62	0.11	0.911
170 3	1.38	4.62	0.30	0.767
170 4	1.26	4.62	0.27	0.787
170 5	0.92	4.74	0.19	0.847
175 1	4.08	4.32	0.95	0.351
175 2	-0.52	4.62	-0.11	0.911
175 3	-1.38	4.62	-0.30	0.767
175 4	-1.26	4.62	-0.27	0.787
175 5	-0.92	4.74	-0.19	0.847

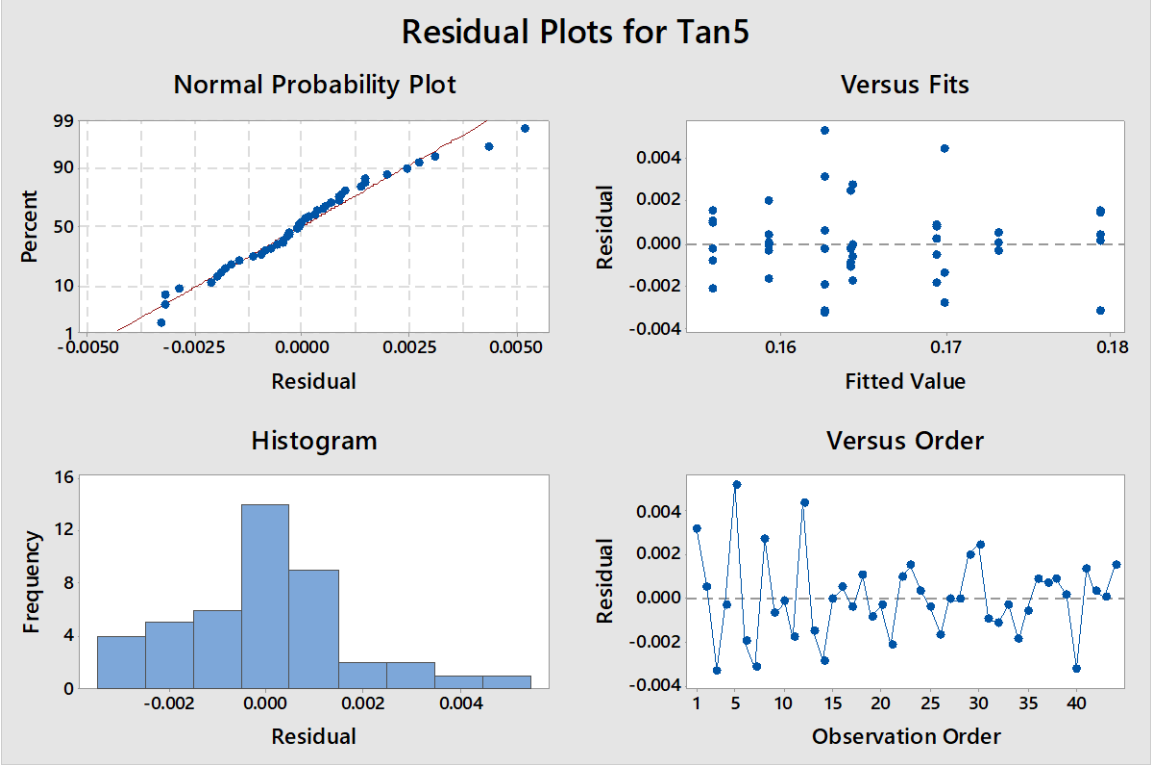

Figure B.13: Residual Plots for Tan Delta with State of Cure and Cure Temperature as Factors

Table B.5: ANOVA Table for Tan Delta

Term	Coef	SE Coef	T-Value	P-Value
Constant	0.166067	0.000327	507.36	0.000
Cure Temp				
170	0.000441	0.000327	1.35	0.187
175	-0.000441	0.000327	-1.35	0.187
State of Cure				
1	-0.006854	0.000617	-11.11	0.000
2	-0.005138	0.000660	-7.79	0.000
3	-0.001820	0.000660	-2.76	0.009
4	0.003608	0.000660	5.47	0.000
5	0.010203	0.000676	15.09	0.000
Cure Temp*State of Cure				
170 1	0.002950	0.000617	4.78	0.000
170 2	0.001215	0.000660	1.84	0.074
170 3	-0.000385	0.000660	-0.58	0.563
170 4	-0.000233	0.000660	-0.35	0.727
170 5	-0.003547	0.000676	-5.25	0.000
175 1	-0.002950	0.000617	-4.78	0.000
175 2	-0.001215	0.000660	-1.84	0.074
175 3	0.000385	0.000660	0.58	0.563
175 4	0.000233	0.000660	0.35	0.727
175 5	0.003547	0.000676	5.25	0.000

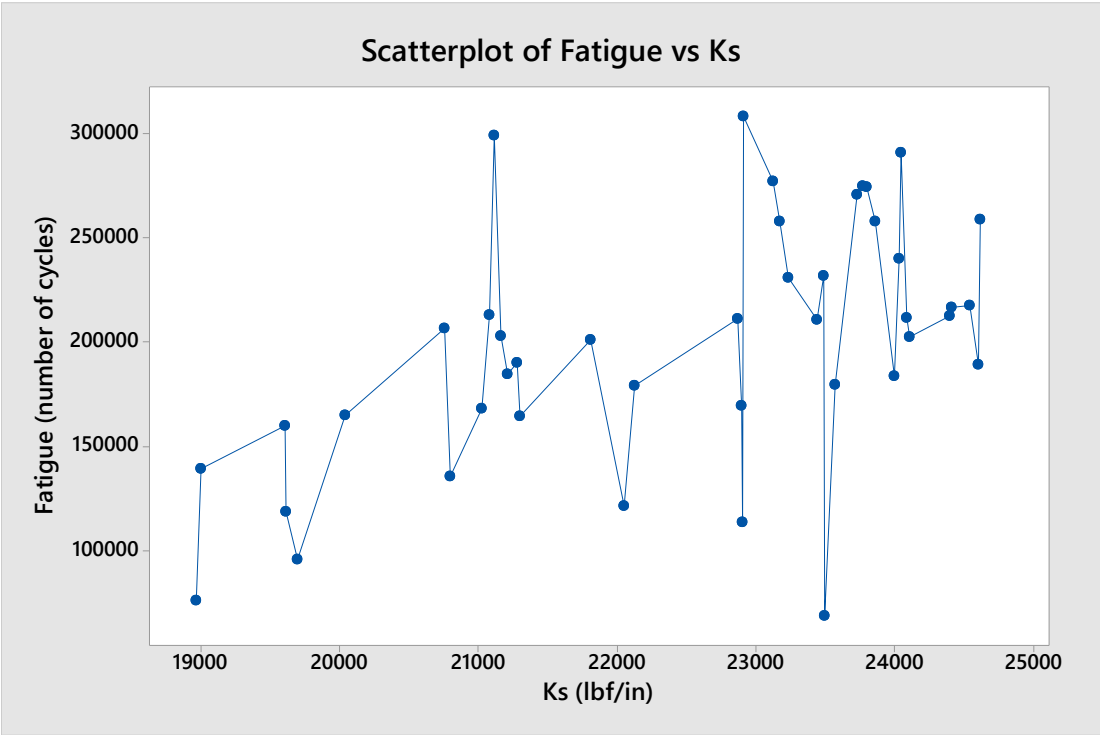

Figure B.14: Fatigue Versus Static Stiffness

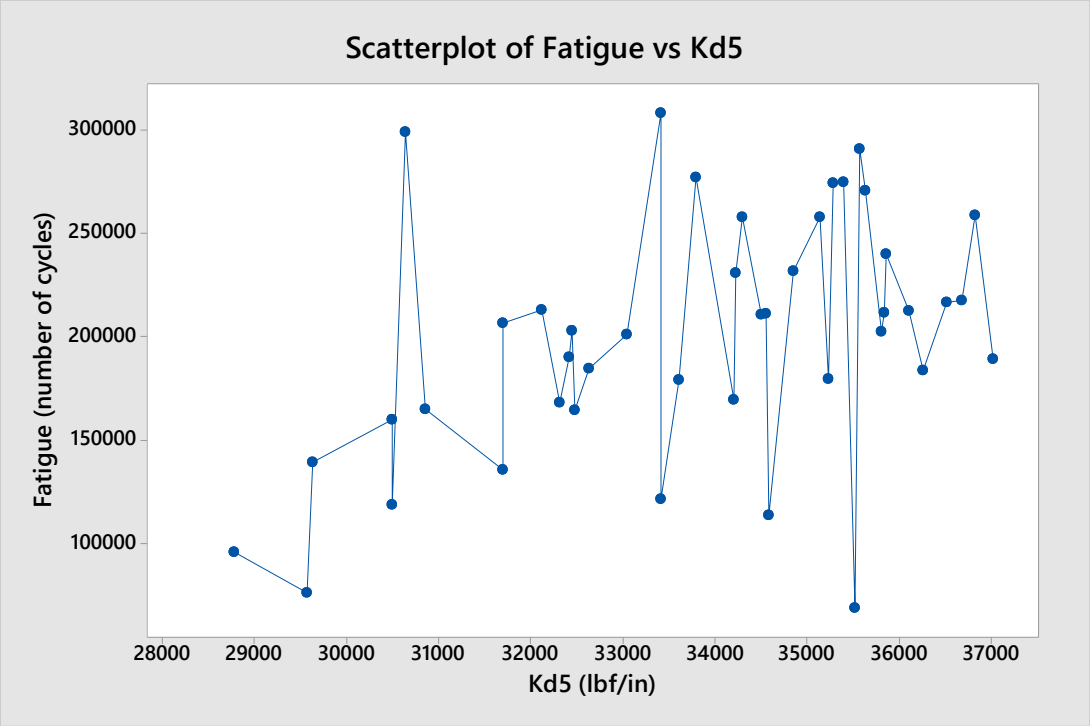

Figure B.15: Fatigue Versus Dynamic Stiffness at 5Hz

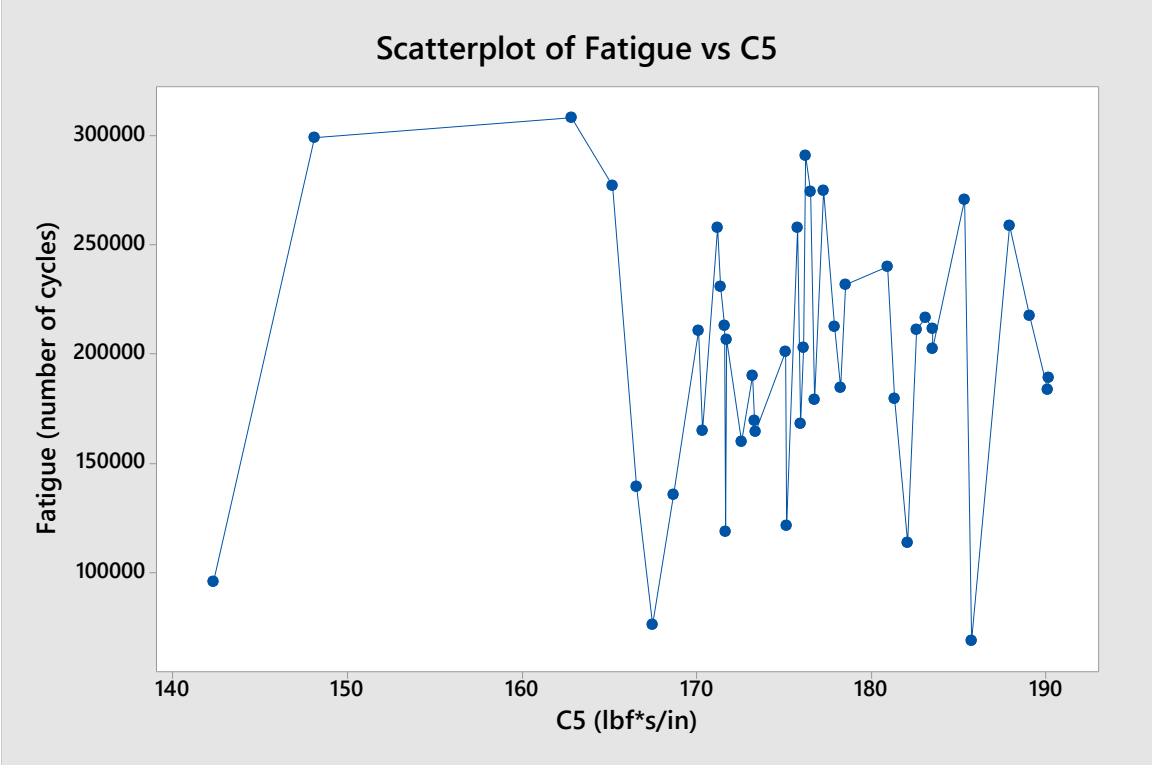

Figure B.16: Fatigue Versus Damping at 5Hz

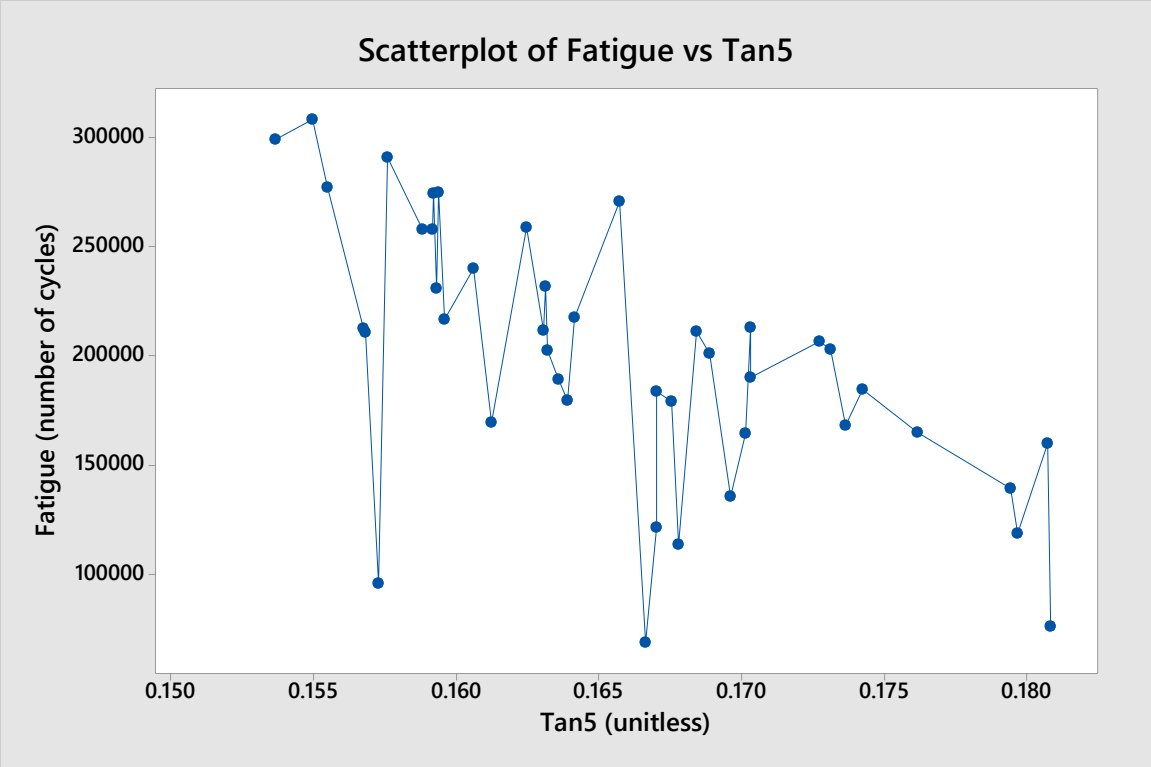

Figure B.17: Fatigue Versus Tan Delta at 5Hz